Old Dominion University
ODU Digital Commons

CCPO Publications | Center for Coastal Physical Oceanography

1999

Modeling the MSX Parasite in Eastern Oyster (Crassostrea virginica) Populations. I. Model Development, Implementation, and Verification

Susan Ford

Eric Powell

John Klinck
Old Dominion University, jklinck@odu.edu

Eileen Hofmann
Old Dominion University, ehofmann@odu.edu

Follow this and additional works at: https://digitalcommons.odu.edu/ccpo_pubs

 Part of the Aquaculture and Fisheries Commons, and the Marine Biology Commons

Repository Citation

Ford, Susan; Powell, Eric; Klinck, John; and Hofmann, Eileen, "Modeling the MSX Parasite in Eastern Oyster (Crassostrea virginica) Populations. I. Model Development, Implementation, and Verification" (1999). *CCPO Publications*. 78.
https://digitalcommons.odu.edu/ccpo_pubs/78

Original Publication Citation

Ford, S., Powell, E., Klinck, J., & Hofmann, E. (1999). Modeling the MSX parasite in eastern oyster (*Crassostrea virginica*) populations. I. Model development, implementation, and verification. *Journal of Shellfish Research, 18*(2), 475-500.

This Article is brought to you for free and open access by the Center for Coastal Physical Oceanography at ODU Digital Commons. It has been accepted for inclusion in CCPO Publications by an authorized administrator of ODU Digital Commons. For more information, please contact digitalcommons@odu.edu.

Journal of Shellfish Research, Vol. 18, No. 2, 475–500, 1999.

MODELING THE MSX PARASITE IN EASTERN OYSTER (*CRASSOSTREA VIRGINICA*) POPULATIONS. I. MODEL DEVELOPMENT, IMPLEMENTATION, AND VERIFICATION

SUSAN FORD,[1] ERIC POWELL,[1] JOHN KLINCK,[2] AND EILEEN HOFMANN[2]

[1]*Haskin Shellfish Research Laboratory*
Rutgers University
Port Norris, New Jersey 08349
[2]*Center for Coastal Physical Oceanography*
Old Dominion University
Norfolk, Virginia 23529

ABSTRACT A mathematical model simulating the host-parasite-environmental interactions of eastern oysters (*Crassostrea virginica*) and the pathogen, *Haplosporidium nelsoni*, which causes MSX disease, has been developed. The model has 2 components. One replicates the infection process within the oyster and the other simulates transmission. The infection-development component relies on basic physiological processes of both host and parasite, modified by the environment, to reproduce the observed annual prevalence cycle of *H. nelsoni*. Equations describing these rates were constructed using data from long-term field observations, and field and laboratory experiments. In the model, salinity and temperature have direct effects upon *in vivo* parasite survival and proliferation as well as on transmission rates. Cold winters depress transmission rates for 1 or 2 years after the event, even if temperatures return to normal. Warm winters have no effect on transmission in subsequent years. Hemocyte activity, parasite density, and the overall environmental quality provided to the parasite by the host also influence the modeled infection process. Hemocytes scavenge and eliminate parasites that die over the winter or that degenerate as a result of failed sporulation. Replication rates of *H. nelsoni* are slowed at high parasite densities. The environmental quality provided by the host, which is a function of oyster food availability and the oyster's potential growth efficiency, affects doubling times and also determines whether the parasite completes its life cycle by forming spores. Spore production is related to a threshold environmental quality, which occurs only in small oysters because of their high growth efficiency. Simulations that use environmental conditions characteristic of Delaware Bay reproduce the observed seasonal *H. nelsoni* cycle, consequent oyster mortality, and spore production in juvenile oysters. The oyster-*H. nelsoni* model provides a quantitative framework for guiding future laboratory and field studies as well as management efforts.

KEY WORDS: *Haplosporidium nelsoni*, numerical modeling, MSX disease, marine pathogen, host-parasite environment

INTRODUCTION

Among the most important influences on population dynamics of eastern oysters, *Crassostrea virginica*, in the United States over the past half century has been disease. Two major diseases, both caused by water-borne protistan parasites, have severely diminished the abundance of natural oyster populations, particularly in the middle Atlantic states (Ford and Tripp 1996). The first to be recognized was Dermo disease, caused by *Perkinsus marinus*. Although it was discovered in the late 1940s in the Gulf of Mexico, it had probably been present throughout the southeastern United States and Gulf of Mexico for many decades (Ray 1996). Between its discovery and 1990, Dermo disease was prevalent only in waters south of Delaware Bay; since then however, epizootic outbreaks have been recorded as far north as Massachusetts (Ford 1996). The second, MSX disease, is caused by *Haplosporidium nelsoni*, a parasite believed to have been introduced to the east coast of the United States, where it began causing epizootic mortalities in Delaware and Chesapeake Bays in the late 1950s and early 1960s. *H. nelsoni* is now present along the entire east coast, although its major impact has been from Virginia north to Maine (Ford and Tripp 1996, Barber et al. 1997).

To synthesize available data and to investigate the factors influencing the interactions of host, parasite, and environment in Dermo disease, mathematical models for *P. marinus* and *C. virginica* were developed (Hofmann et al. 1992, Hofmann et al. 1994, Hofmann et al. 1995). The individual models were then coupled to examine the effects of temperature, salinity, total seston, and food availability on the integrated host-parasite system (Powell et al. 1994, Powell et al. 1996). Simulations indicated that temperature controls on both host and parasite growth rates, and food availability to the oyster, were the major elements influencing the interaction. High oyster reproduction and growth rates in southern latitudes allows populations to withstand Dermo disease pressure much better than in mid-latitudes, where both fecundity and growth rate are lower. Simulations also indicated that an important survival mechanism for the oyster is simply to increase body mass (i.e., growth) at a higher rate than the parasite can proliferate and thus to keep *P. marinus* densities from reaching lethal levels.

In many of the locations where *P. marinus* is present, *H. nelsoni* is also. Particularly in the mid-Atlantic states and along the northeastern coast, both parasites cause major, recurring epizootics. Therefore, to understand the effects of disease on oyster populations in this region, it is necessary to consider the actions and interactions of both parasites on hosts at the individual and population level. Both parasites display distinct seasonal and interannual cycles of infection onset, development, and impact on the host. These cycles are largely a function of environmental factors, primarily temperature and salinity, to which both parasites and the oyster are sensitive. However, the ability to tolerate environmental extremes, or to profit from favorable conditions, is specific to each species. A numerical model offers an effective way to synthesize the many data available for the parasites and their host in a mechanism for understanding the complex interactions among these organisms and their environment.

The objective of this paper is to describe a model developed for *Haplosporidium nelsoni* in oysters. Like that for *P. marinus*, it is a physiological model structured around proliferation and death rates of *H. nelsoni* under different environmental conditions. Equations describing these rates were constructed using data from long-term field observations, and field and laboratory experiments.

The *H. nelsoni* model is described in the following section. The

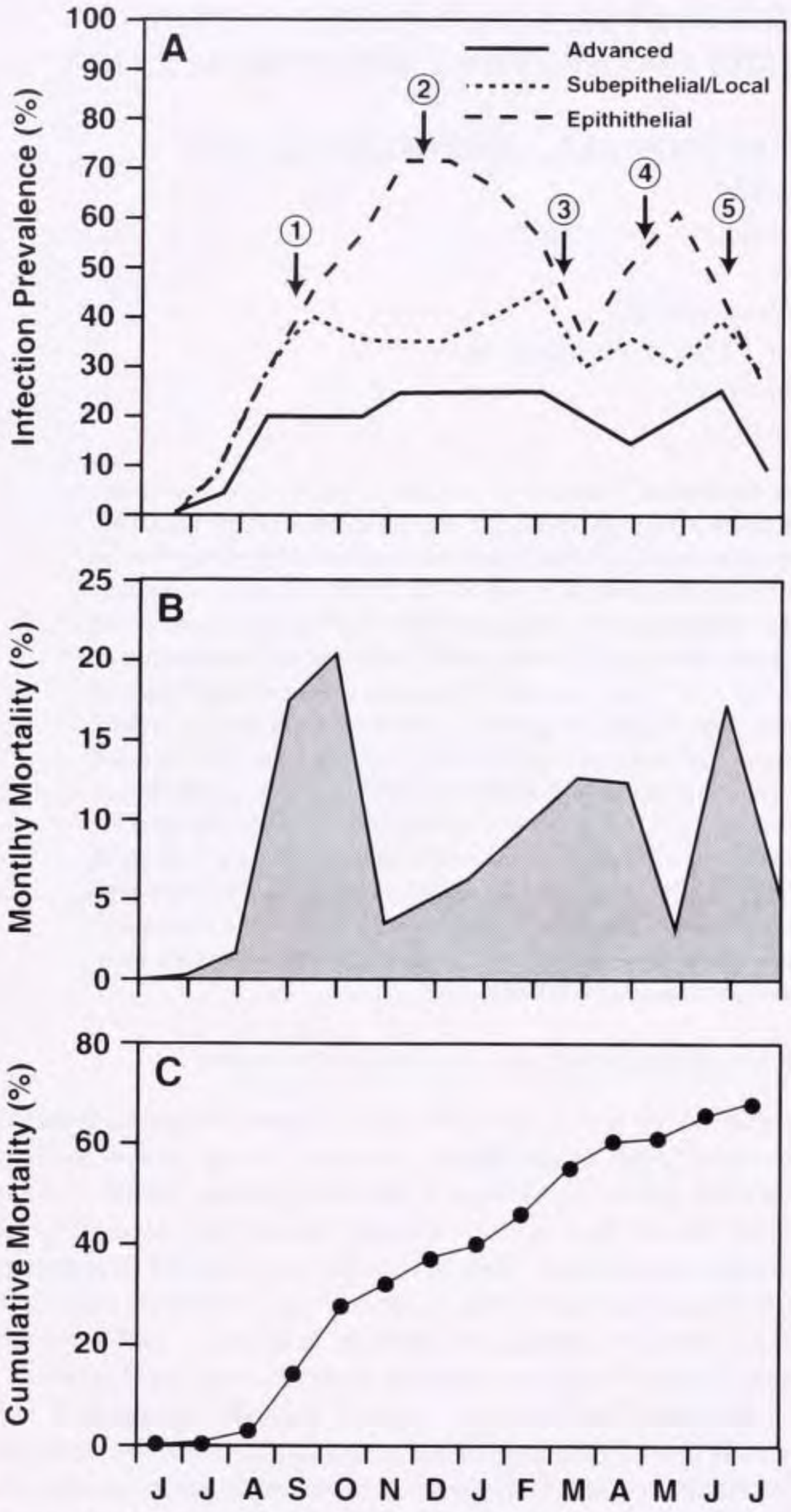

Figure 1. (A) Annual prevalence cycle for *Haplosporidium nelsoni* infections in eastern oysters in Delaware Bay, NJ, (first year of infection) showing relative contributions of epithelial (BFU = 1), subepithelial/local (BFU = 2), and systemic (BFU = 3 & 4) infections to the overall prevalence (see text for definitions). The arrows and numbers indicate different phases of the infection cycle as described in the text. (B) Monthly and (C) cumulative nonpredation mortality for oysters undergoing first year exposure in the same location. Adapted from Ford and Haskin (1982).

succeeding section presents a series of model outputs that illustrate its ability to simulate the seasonal cycle of *H. nelsoni* prevalence and intensity, and consequent oyster mortality, in a high-salinity enzootic area. The model described in the current paper is the basis for the studies presented in two subsequent papers: the effects of varying salinity on MSX disease development (Paraso et al. this volume) and a comparison of the disease in Delaware and Chesapeake Bays with a discussion of the transmission issue (Powell et al. this volume).

METHODS AND MODEL DESCRIPTION

Model Overview

Conceptual Framework

Haplosporidium nelsoni is classified in the phylum Haplosporidia (Corliss 1984, Perkins 1990). In the oyster, it occurs primarily as a multinucleated plasmodium (Ford and Tripp 1996). A second life form, the spore, is found rarely in adult oysters, but can be common in juveniles (R. D. Barber et al. 1991, Burreson 1994). The method of transmission is unknown and may involve another host (Burreson 1988, Haskin and Andrews 1988). To replicate the oyster-*H. nelsoni* interactions, the mathematical model was divided into two principal components. One simulates the infection process within the oyster, including the formation of spores. The second simulates the transmission process, which occurs outside, and independent of, the oyster (Powell et al. this volume).

Within the oyster, observed prevalence and intensity of *H. nelsoni* follows a defined seasonal pattern in all areas where it has been followed closely (Fig. 1a) (Andrews 1966, Farley 1975, Ford and Haskin 1982, Matthiessen et al. 1990). In the mid-Atlantic, infections are acquired from late May/early June through early fall. The earliest recognized stages are plasmodia confined to the gill epithelium. Once established in the epithelium, parasites proliferate, penetrate the basal lamina, and move into the circulatory system where they are carried to all tissues. Acquisition of new infections and *in vivo* parasite proliferation result in rising prevalence and intensity levels throughout the summer and fall (Fig. 1A, point 1), and result in host mortality during late summer and fall. High infection prevalence and intensity occur in the autumn and into the winter, when low water temperatures have slowed the activity of both host and parasite (Fig. 1A, point 2). In late winter and early spring, infection prevalence and intensity decrease, presumably from the degeneration of *H. nelsoni* plasmodia as well as from the deaths of heavily infected oysters (Fig. 1A, point 3). In early spring, infection prevalence and intensity again increase, coincident with rising water temperature, reaching a peak in late May or early June (Fig. 1A, point 4). This peak, which can be the most intense of the annual cycle, is often followed by a dramatic decrease in the number of infected oysters, again linked with the death of heavily infected oysters, but more so with the disappearance of parasites from live oysters (Fig. 1A, point 5). When sporulation occurs, it coincides with both the spring and the fall prevalence/intensity peaks. The *in vivo* component of the *H. nelsoni* model is designed to replicate the above pattern.

To simulate the *in vivo* relationship, the model relies on basic physiological processes of host and parasite to reproduce the complex, bimodal, annual prevalence cycle observed in nature (Andrews 1966, Ford and Haskin 1982). Parasite proliferation, stage transition, and death rates, which are modified by environmental variables both external and internal to the host, form the basis of the model. Salinity and temperature have direct effects upon *in vivo* parasite survival and proliferation (Paraso et al. this volume). They also have both local and regional effects upon transmission. Hemocyte activity, parasite density, and the overall environmental quality provided by the host are additional factors that influence the parasite. The last affects not only parasite doubling times, but whether or not *H. nelsoni* completes its life cycle by producing spores. The environmental quality experienced by the parasite de-

TABLE 1.

Relationship of *Haplosporidium nelsoni* infection categories (see Ford and Haskin, 1982) to range and mean abundance of parasites, expressed in parasites (unit area)$^{-1}$, in tissue selections of infected oysters. Counts were made from oysters with Little Ford Unit (LFU) ratings of 1 to 6 in either gill tissue, visceral mass tissue, or both. In each location, parasites were counted in a total area equalling 64,000 μm^2. The intensity ratings are indicated as Rare (R), Very Light (VL), Light (L), Moderate (M), and Heavy (H). The correspondence between LFUs and Big Ford Units (BFU) is also shown.

INFECTION CATEGORIES			GILL					VISCERAL MASS				
				Epithelial		Subepithelial			Epithelial		Subepithelial	
Distribution	Intensity	BFU	LFU	Range	Mean	Range	Mean	LFU	Range	Mean	Range	Mean
Epithelial	R, VL, L	I	1	0.1–5.4	0.9	0	0	1	0	0	0	0
Subepith/Local	VL, L	II	2	0.5–3.9	1.4	0.1–1.1	0.5	2	0	0	0–0.2	0.1
Systemic	R, VL	III	3	0–1.2	0.3	0.2–0.5	0.3	3	0	0	0.1–0.6	0.4
Systemic	L	III	4	0.2–0.4	0.2	0.2–2.1	1.1	4	0–0.1	0.1	0.5–2.9	1.7
Systemic	M	IV	5	0.4–13.9	5.4	3.0–18.9	8.2	5	0–1.2	0.2	0.6–7.4	3.9
Systemic	H	IV	6	0.3–9.9	3.2	11.9–36.5	20.8	6	0–1.6	0.5	6.8–28.5	17.5

pends, in turn, upon the quantity of food available to the oyster and its potential growth efficiency. Finally, the model simulates deaths of oysters as a consequence of parasitism.

The transmission component of the model is discussed fully by Powell et al. (this volume). Unlike most disease transmission models, including that for *P. marinus*, it does not rely on the density of nearby oysters as a measure of infective parasite concentration. In fact, there is no direct link between spore formation and transmission in the model. Although spores are assumed to be an important element in the life cycle of *H. nelsoni*, it is not known if they are directly infective to other oysters. The infective stage is unknown, but histological observations of infected oysters suggest it is waterborne (Farley 1968, Ford and Haskin 1982). In the model, the relative abundance of these particles is influenced by salinity, on both local and estuary-wide scales, and long-term temperature fluctuations. The infection rate is a function of the abundance of infective particles and the filtration rate of oysters.

This paper focuses on the *in vivo* model, which was constructed by applying rate functions developed from experimental and field data to an overall governing equation that controls the movement of oysters among infection classes according to the parasite load that they have at any time during a simulation. At each step in the construction of this model, output was compared with actual data and modifications implemented, if needed, to fit the model to field observations. To model the cycle in the absence of complete data on host-parasite interactions, and especially transmission, certain assumptions had to be made. The background and biological basis for these assumptions are stated briefly, along with the particular mathematical relationship, and are considered more fully in the Discussion.

Model Units

The first step in developing the *H. nelsoni* model was to define the units that provide the basic reference frame and that allow the model calculations and output to be consistent with measurements and to be compared with observations. The majority of the observations on MSX disease are made by tissue-section histology and make use of scales that categorize *H. nelsoni* infection level according to parasite distribution (local or diffuse) and abundance in the oyster tissue. The scale reflects disease progression in the oyster as infections move from initial light lesions in the gill epithelium to heavy systemic (whole body) infections.

The infection rating system used for the model is based on one developed for studies in Delaware Bay (Ford and Haskin 1982). This semi-quantitative scale involves 3 levels of distribution in the tissue (epithelial, subepithelial/local, and systemic) and 5 levels of abundance (see Ford and Haskin 1982 for details), resulting in a scale of 0 to 15 when the location and intensity for each oyster are multiplied. For reporting and statistical purposes, however, these 15 categories are reduced to 6 or 4, depending on need (Table 1). Similar ratings systems are used in Chesapeake Bay and elsewhere (Farley 1968, Y. Bobo, pers. comm., E. Burreson, pers. comm., R. Smolowitz, pers. comm.).

In contrast to the rating systems in which most observations are reported, the oyster-*H. nelsoni* model is based on the number of parasites per oyster. It was therefore necessary to establish, at the outset, a relationship between parasites per oyster and the semi-quantitative scale. The 0–6 point scale (referred to as Little Ford Units [LFU]) was used as the basis for this relationship because it provided more precision than the 0–4 point scale. The 0–4 point scale was chosen as the final output from the model, however, because it is the simplest, because it can readily be compared with previous publications, and because it is most easily comparable to systems employed by other researchers. These units are referred to as Big Ford Units (BFU) (Table 1). Conversion between the scales simply involves combining the 4 highest LFUs into 2 BFUs for observational use (Table 1); however, the identical mathematical treatment results in a more complex conversion formula. A complete presentation of the conversion system is given below.

Conversion of Infection Categories to Parasite Density

The conversion of the LFU rating system into parasites per oyster was made by selecting archived slides with tissue sections in each of the categories (total n = 50, approximately equally distributed among the 6 categories of infected oyster). Each slide was then re-analyzed using a gridded ocular. All parasites were counted in 40 (40 μm × 40 μm) grids, 20 placed randomly over gill tissue and 20 over the remaining visceral mass. Resulting counts showed that the mean number of parasites per grid in each LFU category was similar for both the gill and the visceral mass (Table 1). The resulting empirical relationship between *H. nelsoni*

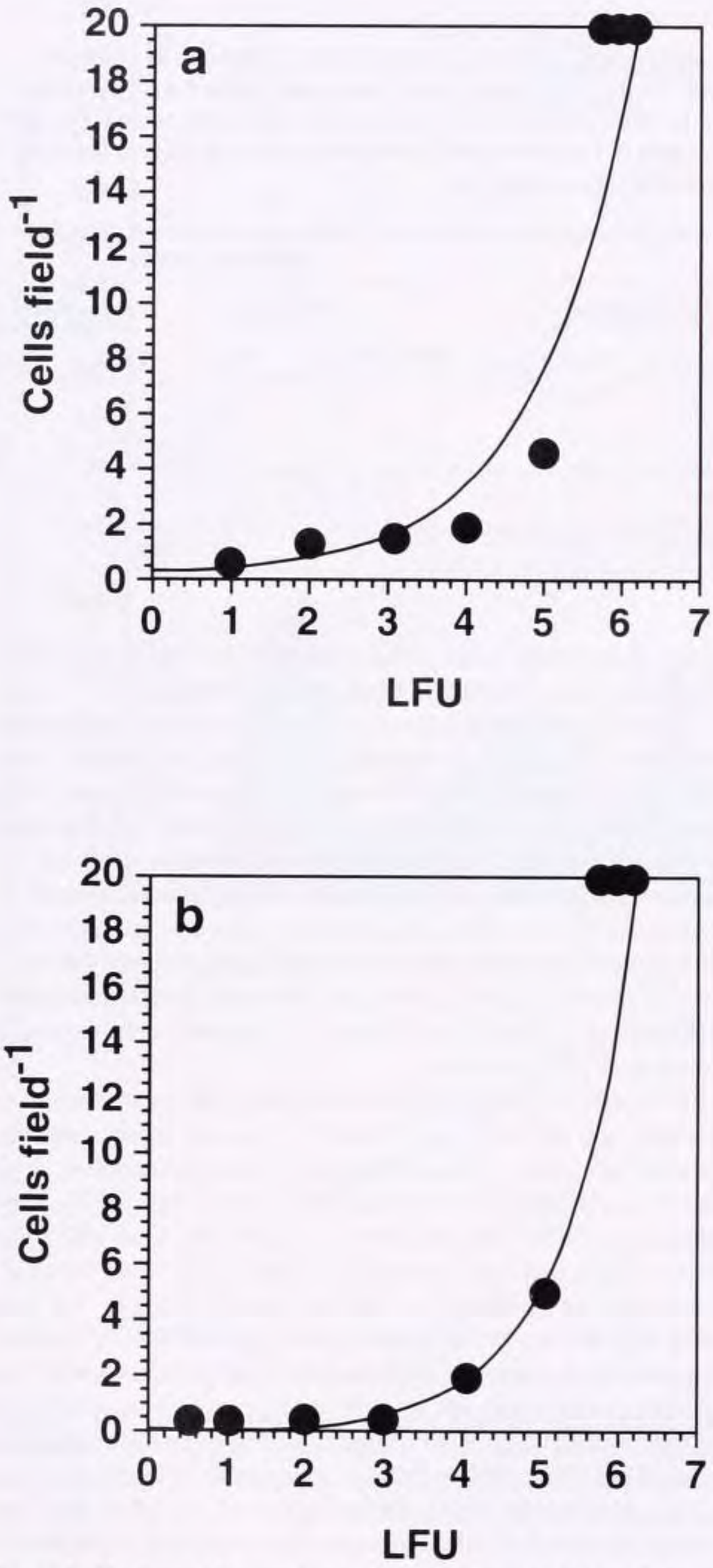

Figure 2. *Haplosporidium nelsoni* plasmodia per 64,000 μm² tissue-section field versus infection intensity categories expressed as Little Ford Units (LFU) for a) epithelial and b) systemic tissues.

infection category and the number of parasites in the oyster was exponential, with a rapid increase in numbers per grid as infections became systemic (LFU 4–6) (Fig. 2a, b). The location of the *H. nelsoni* cells in either epithelial or systemic tissue is included in the final relationship, which is based on a logarithmic scale of the form:

$$LFU = a_{e/s} \ln\left(\frac{C_{e/s}}{bc_{e/s} W_0 frac_{e/s}}\right) \quad (1)$$

where $a_{e/s}$ is a constant that differs for the epithelial (e) and systemic (s) tissue (the notation e/s will be used to denote constants that have different values for epithelial and systemic tissue), $C_{e/s}$ is the number of *H. nelsoni* cells in the epithelial or systemic tissue, b is a scaling in grids per gram wet weight ($gwwt^{-1}$) of oyster tissue, and $c_{e/s}$ is a constant. The coefficients represent the total dry weight in grams ($gdwt^{-1}$) of the oyster tissue (W_0) and the fraction of epithelial or systemic tissue ($frac_{e/s}$) in the animal. The values of the coefficients in equation (1) are given in Table 2.

The method described above for quantifying infection intensity introduced a bias when infections were confined to the epithelium, e.g., LFU 1 (Table 1), because gill epithelium comprised only about 20% of the tissue in each section. Thus, the values obtained in these instances were multiplied by a value of 5 so that the number of parasites per gram tissue was consistent with the values obtained for systemic infections. As a result, the constants a and c vary between the epithelial and systemic conversions and the number of parasites per gram in the epithelial tissue is higher at an equivalent infection intensity than in the systemic tissue (Fig. 2).

The constant b in equation (1) is a conversion from the number of grids counted in a microscope field to the biomass of the tissue counted. In essence, this yields the weight of fixed tissue per grid. The conversion is based on the area of a grid (40 μm × 40 μm), the number of grids counted (40), and the thickness of a tissue cross-section (6 μm). Included in the conversion is a factor of 0.5 to account for the expectation that, on average, an *H. nelsoni* plasmodium would be observed in 2 consecutive cross-sections. The calculation of b also assumes a 10% shrinkage in tissue volume during fixation, thus correcting from fixed to wet tissue weight.

The values for $frac_{e/s}$ are obtained from weights of dissected oysters that show gill tissue to comprise about 20% of the total wet weight (Table 3). Half of this weight was estimated to be epithelium, based on point count stereology of tissue sections. The value for $frac_{e/s}$ was therefore given a value of 0.1.

Rare or very light epithelial infections (LFU = 1) may be identified by as few as 1 or 2 parasites in the gill epithelium in a standard tissue cross-sectional analysis. With this method, however, it is likely that too few parasites are present in some oysters to be detected. Thus, some oysters diagnosed as having no infections (LFU = 0), are undoubtedly infected (Stokes et al. 1995). The model is constructed to reflect this circumstance. The distinction between an uninfected oyster (LFU = 0) and one in the very lightest infection category (LFU = 1) is based on a presumed detection limit and not on the absolute absence of infection. The detection limit, which differs for epithelial and systemic tissue, was obtained from the grid counts described above that were used to convert the infection scale to parasite densities. The lowest level of detection for the conversion counts was 1 *H. nelsoni* cell per 20 grids, with an average value of 0.05 parasite per grid. However, tissue sections are routinely completely scanned for *H. nelsoni* to obtain observed prevalence. Twenty grids (64×10^3 μm^2) represented only an estimated 20% of the gill tissue and 10% of the visceral mass tissue present in a typical section. Therefore, the true detection limit of 1 parasite in either the gill or visceral mass after a complete search of the section would be 1 in 100 grids (= 0.01 $grid^{-1}$) and 1 in 200 grids (= 0.005 $grid^{-1}$), respectively. This translates into 1.3×10^4 and 6.5×10^3 parasites per gram wet weight for gill and visceral mass tissue, respectively.

Model Equations

The model is structured as a two-dimensional array (Figs. 3, 4) with 55 epithelial and 55 systemic infection categories. The infec-

tion level in each category is defined by the average number of *H. nelsoni* in it, with the maximum difference between adjacent classes being 1 population doubling. The difference between infection classes at the higher parasite densities is less than 1 population doubling, because of the nonlinear distribution of LFUs with respect to parasite number (Fig. 2). The nonlinear arrangement was required to provide multiple infection classes within each LFU infection category and, consequently, necessitated scaling the transfers between infection categories by the ratio of the parasite cell number (C) between adjacent classes as:

- for transfers up in epithelial tissue: $C_e/(C_{e+1} - C_e)$
- for transfers down in epithelial tissue: $C_e/(C_e - C_{e-1})$
- for transfers up in systemic tissue: $C_s/(C_{s+1} - C_s)$
- for transfers down in systemic tissue: $C_s/(C_s - C_{s-1})$.

For simplicity, these scalings are not explicitly stated in the equations given below. In this array, only the [0,0] infection class is truly uninfected; however, a larger portion of the array contains infections not detectable by the tissue-section diagnostic method in which the model output is reported. To establish the boundaries of the patently uninfected class, LFU = 0, in the $e \times s$ array, the limits of detection described earlier were used to solve equation (1) and the array steps characterized by parasite densities below that value were defined as uninfected. For example, for a 1-g oyster, epithelial classes with LFUs ≤ 0.8 and systemic classes with LFUs < -1.6 contained parasites below the detection limit. The lower LFU limit for systemic tissue originates from the much larger tissue cross-section area searched for the parasite, as discussed previously.

The governing equation for determining the prevalence and intensity of *H. nelsoni* infections in the epithelial (e) and systemic (s) tissue of oysters (O) is given by:

$$\begin{aligned}\frac{dO_{e,s}}{dt} = &- \alpha_{e,s}O_{e,s} - \beta_{e,s}O_{e,s} + \alpha_{e,s-1}O_{e,s-1} + \beta_{e-1,s}O_{e-1,s} \\ &+ \alpha_{e,s+1}O_{e,s+1} + \beta_{e+1,s}O_{e+1,s} - M_{e,s}O_{e,s} - \gamma_{e,s4}\,O_{e,54} \\ &+ \delta_{e_1}\,\delta_{s_0}\,\frac{1}{2}\sum_{s=s_4}^{N}\sum_{e=0}^{N}\gamma_{e,s}O_{e,s} \qquad (2)\end{aligned}$$

where the first 6 terms represent the movement of oysters between infection intensity classes through gains or losses of *H. nelsoni* cells in the epithelial and systemic tissue (Figs. 3, 4). The coefficients, α and β, determine the rate at which parasites are gained or lost. The parameterizations used to determine these coefficients are given in the following sections. The seventh term in equation (2) represents the loss of parasites through oyster mortality from lethal infections as determined by the rate of mortality, M. The final 2 terms in equation (2) represent the transfer of oysters from heavy infection classes to lower infection classes due to the formation or attempted formation of spores by *H. nelsoni* in the oysters with advanced infections, which results in a loss of oysters from BFU category 4 (s_4 in equation 2), and a gain of infected oysters into infection class [1,0]. The δ functions represent a step-function process in which the oysters are introduced into the [1,0] infection class only (Fig. 3). The coefficient γ determines the rate of this transfer process.

The establishment of infection in uninfected oysters ([0,0] class) is determined by the equation:

$$\frac{dO_{00}}{dt} = -\beta_{0,0}O_{0,0} + \frac{1}{2}\delta_{e,0}\delta_{0,s}\sum_{s=s_4}^{N}\sum_{e=0}^{N}\gamma_{es}O_{es} \qquad (3)$$

where the first term represents the acquisition of *H. nelsoni* infective particles at a rate determined by $\beta_{0,0}$. The second term represents addition of oysters to the uninfected class after hypothesized abortive *H. nelsoni* sporulation events (see Section e), as given by the eighth term in equation (2). These oysters are divided evenly between the [0,0] and [1,0] infection classes, as given by the last terms in equations (2) and (3).

For the sake of simplicity and broad application, the 0–4 category BFU scale was chosen for the model output. Parasite numbers are converted into BFUs (Fig. 4) and model simulations report the proportion of oysters in each of the BFU categories. Certain rules apply to the movement of oysters among infection categories, all based on histological observations of the disease process (Farley 1968, Ford and Haskin 1982). To reflect the fact that infections are initiated in the gill epithelium, uninfected oysters [0,0 class] must move first into an epithelial class before entering a systemic class (Figs. 3, 4). Oysters never reach high epithelial infections, $LFU_e > 6.5$, without developing systemic infections, and this is modeled by an appropriately calibrated transfer function as discussed later. Oysters in systemic classes ≥ 7.0 are automatically placed in the dead oyster category because parasite densities represented by these classes are higher than those found in live oysters. Additional mortality processes will be discussed later.

The diagonal line separating BFU 2 and BFU 3 (Fig. 4) is based on the observation that BFU category 2 is normally reached when advancing epithelial infections (BFU 1) give rise to local systemic infections (BFU 2), which then expand into BFU 3 and then BFU 4. BFU category 3 also includes infections decreasing in intensity. In the latter, parasite burdens diminish simultaneously in epithelial and systemic tissues, hence oysters move in a diagonal toward the undetectable infection category (BFU 0) rather than back through BFU 2 to BFU 1.

Proliferation of *H. nelsoni*

Transfers of oysters to different infection intensity classes are assumed to be due to proliferation and death of *H. nelsoni* cells, except in two cases. First, the acquisition of initial infections is determined by an external factor termed "transmission" ($\beta_{0,0}$ in equation 3). Second, the development of an epithelial into a systemic infection is determined by an invasion rate that is not simply a function of cell division. These transfers are discussed in the following section and a schematic showing the many linkages in the oyster-*H. nelsoni* model is given in Fig. 5. To more easily describe the sequence of processes involved, the model is described as it simulates the yearly infection cycle (Fig. 1A) beginning with the onset of infection in June.

Temperature-dependent proliferation of H. nelsoni. After the acquisition of *H. nelsoni* infections in early June (Fig. 1A), the proliferation of plasmodia in the epithelial and systemic tissue ($g_{e/s}(T)$) is assumed to be exponential with a doubling rate that is modified by temperature as:

$$g_{e/s}(T) = b_{0_{e/s}}\,e^{d(T-T_0)} \qquad (4)$$

where $b_{0_{e/s}}$ is the proliferation rate of the parasite in epithelial or systemic tissue based on a doubling time at a reference temperature, T_0. The reference temperature was taken as 15 °C instead of the standard 20 °C, because 20 °C did not produce adequate parasite division rates in the summer as compared to field observations.

TABLE 2.

Definition, units, and values for the variables used in the oyster-*H. nelsoni* model equations. Delaware Bay and Chesapeake Bay are abbreviated DB and CB, respectively.

Variable	Definition	Units	Value
a_e	constant	none	1.244
a_s	constant	none	0.919
$C_{e/s}$	epithelial or systemic *H. nelsoni* cells	number of cells	calculated
b	scale factor	grids (g wet wt)$^{-1}$	1.3×10^6
c_e	constant	cells (grid)$^{-1}$	0.135
c_s	constant	cells(grid)$^{-1}$	0.022
W_0	oyster dry weight	g	chosen
frac$_e$	fraction of W_0 that is epithelial tissue	none	0.1
frac$_s$	fraction of W_0 that is systemic tissue	none	0.9
α	growth rate	d^{-1}	calculated
β	growth rate	d^{-1}	calculated
$g_e(T)$	temp dependent parasite growth rate in epithelium	d^{-1}	calculated
g_s(T)	temp dependent parasite growth rate in systemic tissue	d^{-1}	calculated
b_{0e}	doubling time of parasite in epithelial tissue	d^{-1}	0.23105
b_{0s}	doubling time of parasite in systemic tissue	d^{-1}	0.69315
d	temperature effect on growth rate	°C^{-1}	0.04
T_0	parasite growth rate reference temperature	°C	15
crowd$_{e/s}$	density-dependent control on growth	none	calculated
*I*Factor	oyster ingestion factor	none	calculated
*c*crowd$_e$	epithelial cell threshold for crowding	number of cells (g dry wt)$^{-1}$	2.5×10^6
*c*crowd$_s$	systemic cell threshold for crowding	number of cells (g dry wt)$^{-1}$	3.3×10^5
cp	rate of increase of crowding effect	none	1.5
d_0	base cell diffusion rate	d^{-1}	0.138
DD	degree days	°C d	calculated
Δ°	temperature differential	°C	calculated
SM_e	maximum rate of cold susceptibility in epithelial tissue	none	2.0
SM_s	maximum rate of cold susceptibility in systemic tissue	none	8.0
k_e	*DD* value at which reach one-half SM_s	°C d	20.0
k_s	*DD* value at which reach one-half SM_e	°C d	10.0
SD_e	susceptibility decay factor in epithelial tissue	(°C d)$^{-1}$	0.2
SD_s	susceptibility decay factor in systemic tissue	(°C d)$^{-1}$	0.1

TABLE 2.

continued

Variable	Definition	Units	Value
HR(*T*)	temperature dependent hemocyte rate	d^{-1}	calculated
hr_0	hemocyte activity base rate	d^{-1}	0.278
θ	hemocyte activity temperature rate	(°C)$^{-1}$	0.08155
Th_0	hemocyte activity base temperature	°C	20.0
crowd$_{eh}$	epithelial cell threshold for crowding for hemocytes	cells (g dry wt)$^{-1}$	3.0×10^6
*eh*crowd	hemocyte crowding threshold in epithelial tissue	none	calculated
$NGER_0$	threshold value for modified net production	(g dry wt)$^{-1}$	0.25
$NGER_{d0}$	minimum potential growth efficiency	none	0.25
$NGER_{q1}$	minimum accumulated potential growth efficiency needed for sporulation	(g dry wt)$^{-1}$	100
$NGER_{q2}$	minimum accumulated potential growth efficiency needed for attempted sporulation	(g dry wt)$^{-1}$	10
SSR	spore susceptibility decay rate	d^{-1}	0.1151
Spore*S*	sporulation rate	d^{-1}	calculated
SporeS_d	sporulation rate modifier	none	set at 1.0 or calculated
SST_0	spore temperature susceptibility	°C	15
SST_{sp}	susceptibility temperature switch	°C	2.64
Temp*SS*	spore temperature susceptibility factor	d	none
*Sp*Frac	fraction of *H. nelsoni* cells undergoing	(oyster)$^{-1}$	0.25
Total*S*	spores released	cells	calculated
Spore*N*	number of spores formed per plasmodium	number (cell)$^{-1}$	25
Spore$_k$	oyster death rate from sporulation	d^{-1}	0.1733
*S*mort	salinity mortality factor	none	calculated
SD_1	salinity mortality factor	none	103.0
SD_2	salinity mortality factor	none	0.24065
SD_3	salinity mortality factor	(ppt)$^{-1}$	0.592456
SD_4	salinity halving time	d	4.0
*S*death	salinity mortality rate	d^{-1}	calculated
*S*factor	salinity effect of growth	none	calculated
sg	salinity effect on growth	(ppt)$^{-1}$	0.4605
S_0	salinity growth effect reference salinity	ppt	15.0
*S*death$_{max}$	maximum salinity mortality rate	d^{-1}	0.01787

continued on next page

TABLE 2.

continued

Variable	Definition	Units	Value
Sdiff	salinity effect on diffusion rate	none	calculated
*SF*1	salinity diffusion constant	none	9.0
*SF*2	salinity diffusion constant	none	2.65
*SF*3	salinity diffusion constant	ppt	3.0
Mort*O*	mortality rate	d^{-1}	calculated
*M*span	mortality time span	d	30
Ma	mortality constant	none	0.00747
Mb	mortality constant	$(LFU)^{-1}$	0.717
*I*1	infection constant	none	0.0231
*I*2	infection constant	none	1×10^{-4}
*I*3	infection constant	min $particle^{-1}$	–0.9
*IP*filter	infective particles filtered	particles min^{-1}	calculated
*IP*conc	infective particle concentration	particles l^{-1}	calculated
filt	oyster filtration rate (Hofmann et al. 1992)	l min^{-1}	calculated
*IP*temp	infection temperature effect	none	calculated
*IP*sal	infection salinity effect	none	calculated
*IP*season	infection seasonal effect	none	chosen
SM_1	salinity mortality constant	ppt	1.6
SM_2	salinity mortality constant	none	11.0
SM_0	salinity mortality reference salinity	ppt	17.0
IP_{conc_0}	base infective particle concentration	particles l^{-1}	450 (DB, 1960s) 750 (DB, 1980s) 450 (CB)
*IP*salrate	rate of change in spore concentration	d^{-1}	calculated
$IP\text{salrate}_0$	change in spore concentration reference rate	d^{-1}	0.038376
$IPsal_0$	change in spore concentration base salinity	ppt	15.5
S_{IP}	salinity values from a specified time series for salinity oscillations	ppt	chosen
$IPsal_1$	change in spore concentration salinity constant	ppt	5.0
$IPconc_{max}$	maximum conc. of infective particles	particles l^{-1}	900 (DB, 1960s) 1500 (DB, 1980s) 900 (CB)
$IPconc_{min}$	minimum conc. of infective particles	particles l^{-1}	0.001
*DD*10	transmission degree days	°C	calculated
DD_0	transmission degree day reference level	°C	700 (DB) 520 (CB)
DD^1	transmission degree day constant	°C	20.0
DD_2	transmission degree day constant	none	1.6
$IP\text{temp}_{est}$	estimated effect of degree day on infective particle concentration	none	calculated

The rate at which the proliferation rate is modified by temperature is given by *d*, which is based on a Q_{10} of 3.2. This is also derived from the requirement to obtain adequate division rates in the summer. Data taken from field observations in the lower Chesapeake Bay were used to fit the model-derived simulations (Andrews 1966).

Proliferation rates differ for parasites in the epithelial and the systemic tissue because simulations using the same base rate for both tissues did not accurately reproduce field observations. Thus, it was necessary to assume doubling times of 1 and 3 days for the plasmodia in the systemic and epithelial tissue, respectively (Fig. 6). The biological rationale for the faster reproduction of systemic parasites is that they are continuously bathed in hemolymph, which should provide better nutrition than that received by parasites in the epithelium, where parasites are lodged between cells (Myhre 1973).

Density-dependent proliferation of H. nelsoni. The *H. nelsoni* cell division rates given by equation (4) are sufficient to simulate the observed increase in infection prevalence and intensity after the initial infection in June (Fig. 1A, point 1). However, the reduced proliferation rates and plateauing of infection levels observed in late fall and early winter (Fig. 1A, point 2) could not be simulated with a simple reduction in doubling rate resulting from decreasing temperatures. Therefore, an additional mechanism was indicated and this was assumed to be a decrease in *H. nelsoni* replication rate due to parasite density-dependent effects as has been previously described for *P. marinus* (Saunders et al. 1993, Hofmann et al. 1995). During summer and fall, parasite numbers in oysters have steadily increased and this biological control on proliferation rates occurs as parasite density approaches the carrying capacity of the environment (in this case oyster tissue). The density-dependent control is related to oyster size and *H. nelsoni* cell density as:

$$crowd_{e/s} = min\left[1, \left(\frac{I\text{factor}(j)\ ccrowd_{e/s}\ W_0(j)\ frac_{e/s}}{C_{e/s}}\right)^{cp}\right] \quad (5)$$

where *j* indicates oyster size in g dry weight, *I factor(j)* is a size-dependent factor determined by oyster ingestion rate (discussed subsequently) and $ccrowd_{e/s}$ is the concentration of *H. nelsoni* cells in either the epithelial or systemic tissue at which crowding begins. The crowding effect in systemic tissue becomes important at parasite numbers that are about a factor of 10 lower than those in the epithelial tissue (Fig. 7) and the cell densities (Table 2) at which this effect becomes important were determined by comparison of simulated output to field observations on infection intensification.

TABLE 3.

The average wet weight (AWW), standard deviation (STD), standard error (SE), minimum and maximum wet weight ranges, and percent of the total tissue for dissected oyster tissues (n = 103 oysters).

Tissue	AWW (g)	STD (g)	SE (g)	Minimum (g)	Maximum (g)	Percent (%)
Mantle	1.666	0.539	0.053	0.7	4.0	19
Digestive Gland	1.715	0.55	0.054	0.7	4.0	19
Gill	1.56	0.382	0.038	0.6	2.5	18
Adductor Muscle	1.677	0.549	0.054	0.6	3.2	19
Remainder	2.282	1.017	0.1	0.4	6.0	26

Diffusion between Epithelial and Systemic Tissue

The crowding effect given by equation (5) modifies the temperature-dependent proliferation rates given by equation (4) to provide the final doubling times of *H. nelsoni*. These rates apply to *H. nelsoni* proliferation in all epithelial and systemic tissues, but not to the transfer of parasites from epithelial to systemic tissue. Although the mechanism by which *H. nelsoni* penetrates the basal lamina is not known, for purposes of the model, this transfer is assumed to be governed by a one-way diffusion process; i.e., plasmodia diffuse from the epithelial tissue to the systemic tissue. This process is described by an empirical equation of the form:

$$diffusion = d_0\, max\left(0, \sqrt{\frac{C_e - \frac{C_s frac_s}{frac_e}}{C_{e=55}}}\right) \quad (6)$$

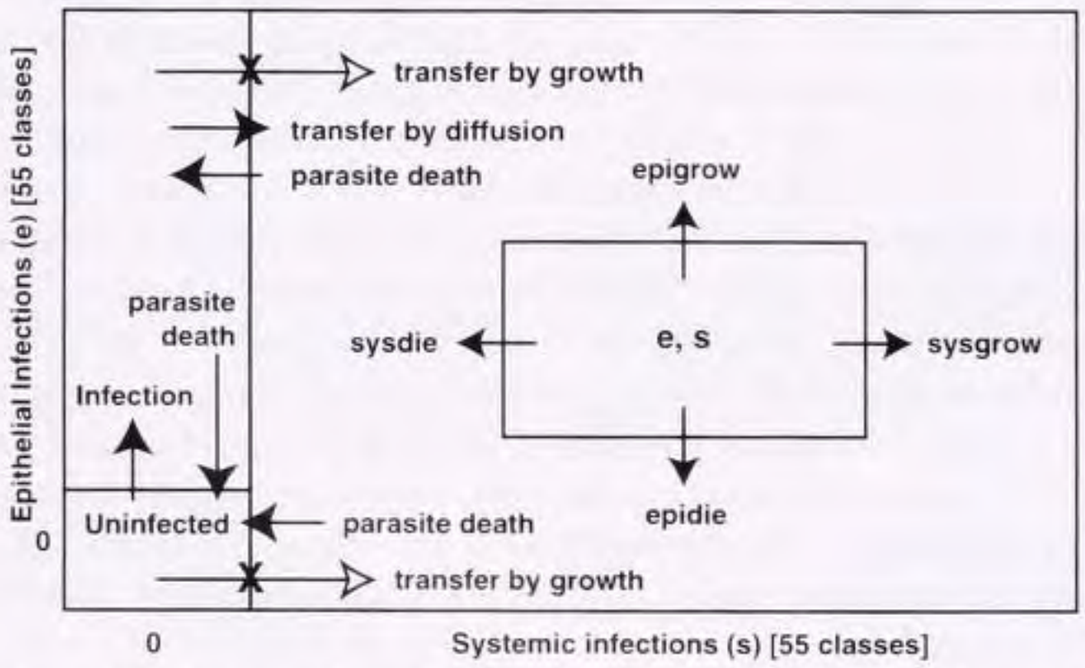

Figure 3. Conceptual model showing possible transfers of oysters through systemic (s) and epithelial (e) infection classes. The relative parasite density in each class is determined by the proliferation (epigrow and sysgrow) or death (epidie and sysdie) of *Haplosporidium nelsoni*. The [0,0] class represents uninfected oysters. Oysters cannot transfer from the uninfected class directly to a systemic infection class (open arrow with X), but must pass into an epithelial class first (i.e., initial infections are established in the epithelium), as indicated by the vertical arrow. Oysters may transfer to the uninfected class when the parasites die (horizontal and vertical arrows). Transfer of an oyster from an epithelial infection class into a systemic infection class is governed by the diffusion (horizontal arrow), not proliferation (open arrow with X), of parasites across the epithelial barrier. Oysters may transfer from systemic to epithelial infection levels by parasite death.

in which the transfer rate depends on the density of parasites in both epithelial and systemic tissues. Equation (6) results in increased diffusion (or invasion) of *H. nelsoni* to systemic tissue as the number of parasites in the epithelial tissue increases (Fig. 8). Equation (6) applies to all transfer from epithelial to systemic tissue; however, there can be no transfer from the truly uninfected compartment (0,0 class) directly to the systemic compartment. Only an epithelial infection can give rise to a systemic infection (Fig. 3).

From the above, the equations for proliferation of *H. nelsoni* in epithelial (G_e) and systemic (G_s) tissue become:

$$G_e = g_e(T)\, crowd_e \quad (7)$$

$$G_s = g_s(T)\, crowd_s\, diffusion. \quad (8)$$

Thus, the basic rate of *H. nelsoni* infection development includes only temperature- and density-dependent effects on doubling time, plus a diffusive contribution of parasites to the systemic tissue.

H. nelsoni Mortality

H. nelsoni prevalence and intensity decreases in early spring (Fig. 1A, point 3). Although many of the most heavily infected oysters die at this time, it is evident from histological observations that parasites are also in poor condition and probably dying (Ford and Haskin 1982). In the model, this loss of parasites cannot be accounted for by a simple reduction in *H. nelsoni* doubling rate at low winter temperatures or by a direct effect of cold temperatures

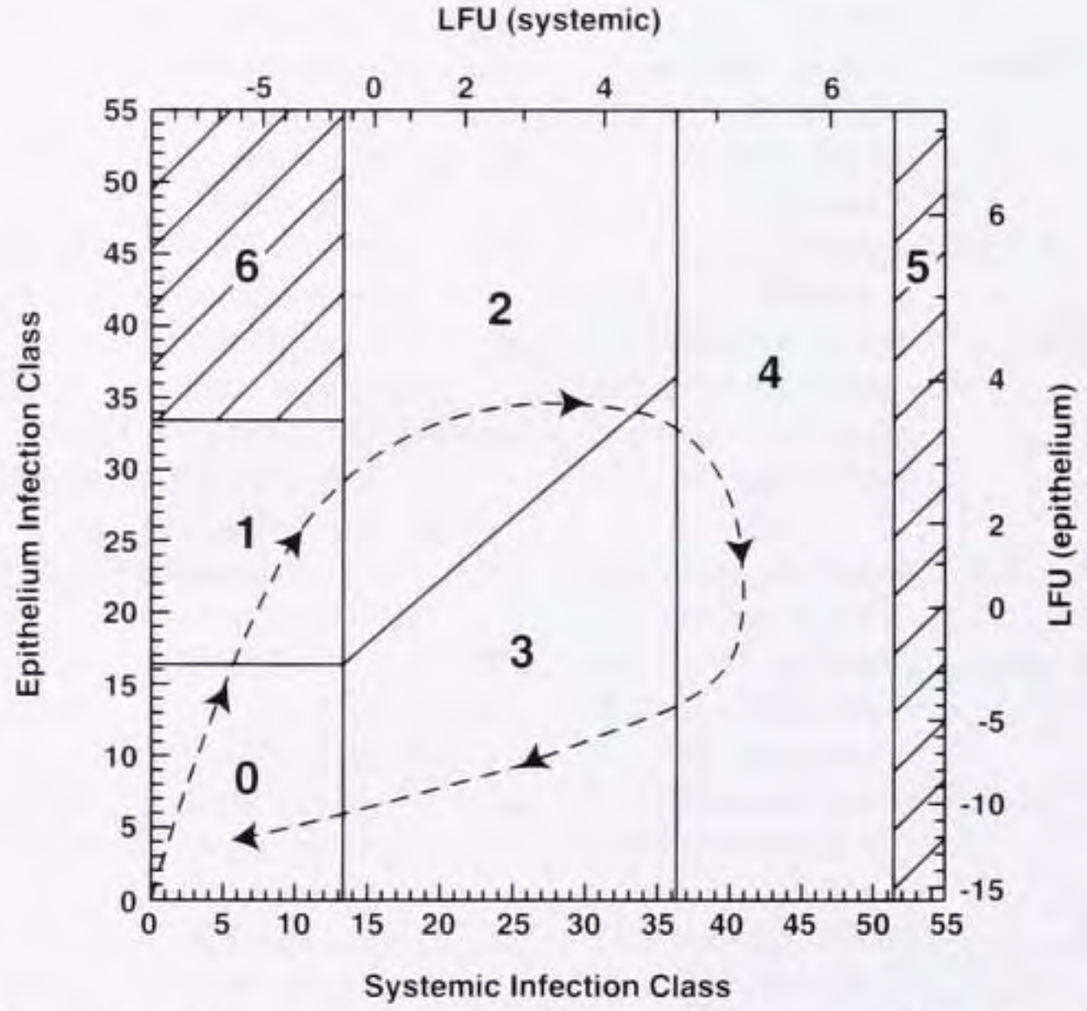

Figure 4. Schematic showing the relationship between the systemic and epithelial infection classes used in the oyster-*H. nelsoni* model and Little Ford Units (LFU). Model infection classes (0–55) for epithelial and systemic infections are shown on the left and bottom sides of the figure, respectively. Their respective LFU categories (0–6) are shown on the right and top sides. The model output is in LFUs, but these are converted to Big Ford Units (BFU) for plotting. BFUs are shown as areas within the plot, with numbers from 0–6. The cross-hatched regions indicate infection levels where the oysters are dead (BFU = 5) or epithelial infection levels that are not normally achieved in nature (BFU = 6). BFU category 0 represents infections that are below the level of detection. The dashed arrows indicate the *H. nelsoni* infection trajectory normally observed in oysters during infection proliferation and remission.

on *H. nelsoni* survival. Simulations of both conditions failed to agree with field observations. In fact, the decrease occurs at a time when temperatures are rising.

Obviously, an additional factor is operating in nature to cause the observed decrease in parasite density. Simulations agreed with observations when it was assumed that the spring decrease in parasite density is due to a combination of 2 factors: 1) *in vivo* conditions coinciding with low winter temperatures that debilitate *H. nelsoni* plasmodia and increase their susceptibility to hemocyte attack; and 2) increasing activity of oyster hemocytes in the spring that removes the damaged parasites. In addition to the apparent degeneration of parasites in late winter, the biological rationale includes experimental data showing that oyster hemocytes do not attack and phagocytose live *H. nelsoni*, but readily ingest killed parasites or those with arrested metabolism (Ford et al. 1993, Ford and Ashton-Alcox 1998). The exact mechanism that results in reduced viability of *H. nelsoni* is unknown, but for convenience, the term "cold" susceptibility is used for this factor.

Cold susceptibility. The susceptibility of *H. nelsoni* to low temperature was assumed to depend on the number of winter days during which the parasites are exposed to temperatures below a threshold (i.e., degree days). The number of degree days (*DD*) was determined by summing the difference between the threshold temperature and the ambient temperature (Δ°) over time as:

$$DD = \sum_{min=0}^{max200} \Delta^\circ dt \tag{9}$$

where *DD* ranges between 0 and 200. The threshold temperature was taken to be 5 °C, based on simulations covering a range of temperatures between 0 °C and 10 °C. As long as Δ° was positive (ambient temperature declining), the number of degree days was related to *H. nelsoni* susceptibility to oyster-hemocyte attack in epithelial and systemic tissue ($HSus_{e/s}$) as:

$$HSus_{e/s} = \frac{SM_{e/s}\, DD}{k_{e/s} + DD} \tag{10}$$

This hyperbolic saturation relationship results in increasing susceptibility of *H. nelsoni* to oyster hemocytes as cold exposure is prolonged. However, above a certain level of cold exposure, susceptibility no longer increases (Fig. 9). In the model, parasite burdens are made to diminish more rapidly in the systemic tissue than in the epithelium to match histological observations that, as infection intensity diminishes, the last parasites seen are in the epithelium (Ford and Haskin 1982, Ford 1985a). The data imply that parasites are eliminated faster from systemic locations and the biological rationale assumes that the number of hemocytes per parasite is higher in the circulation (systemic tissue) than in the epithelium and therefore the rate at which moribund parasites can be scavenged by the hemocytes is greater.

As temperatures increase in the spring, the degree-day value decreases and eventually becomes negative. During this time, the assumption is that susceptibility of *H. nelsoni* plasmodia to the oyster hemocytes decreases as parasites recover from cold exposure, or because only undamaged parasites remain. This effect is incorporated into equation (10) through the addition of a term that attenuates *H. nelsoni* cold susceptibility as temperature increases:

$$H\ Decay = \frac{1 + \Delta^\circ\, SD_{e/s}}{1 - \Delta^\circ\, SD_{e/s}} \tag{11}$$

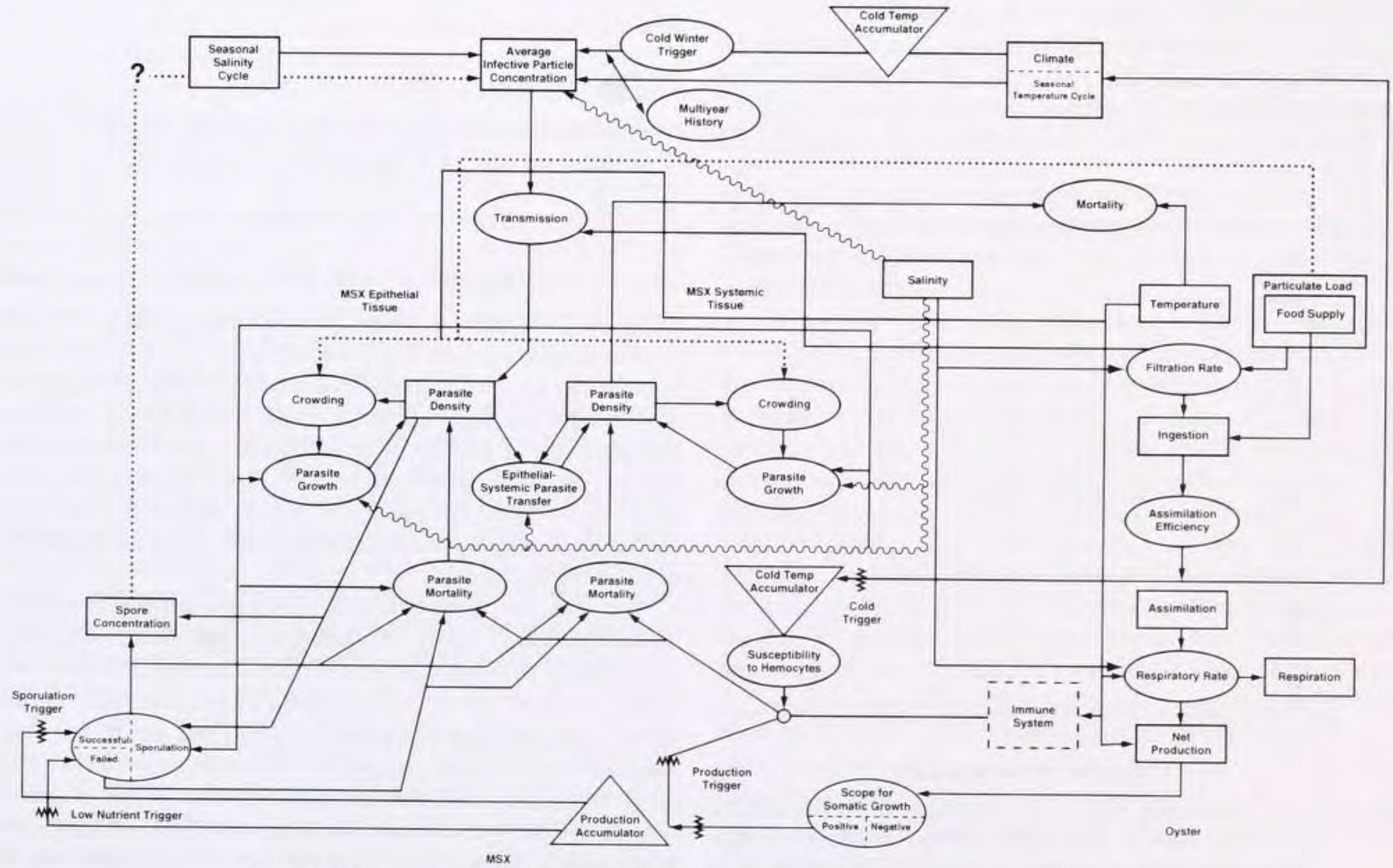

Figure 5. Schematic of the linkages and processes included in the oyster-*H. nelsoni* model.

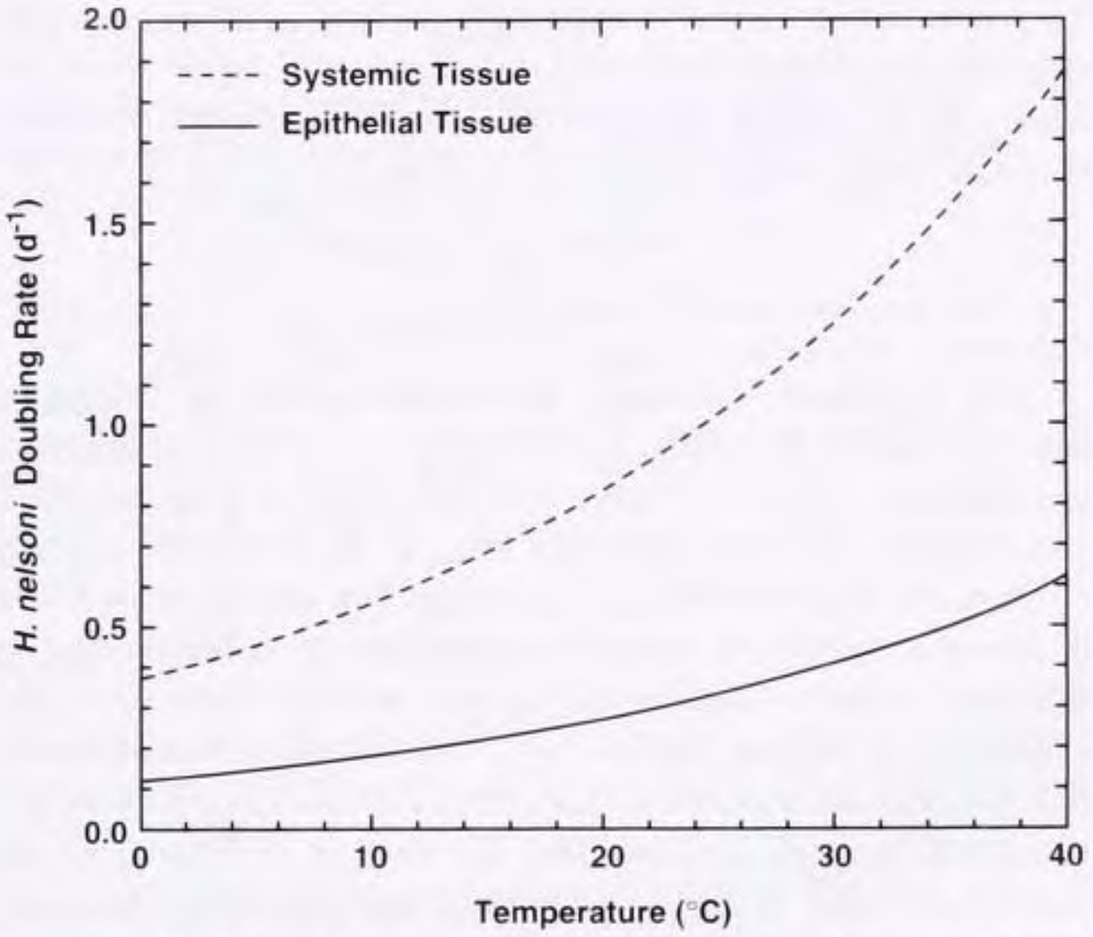

Figure 6. *Haplosporidium nelsoni* proliferation rates in epithelial and systemic tissues of oysters as a function of temperature at salinities ≥ 15 ppt.

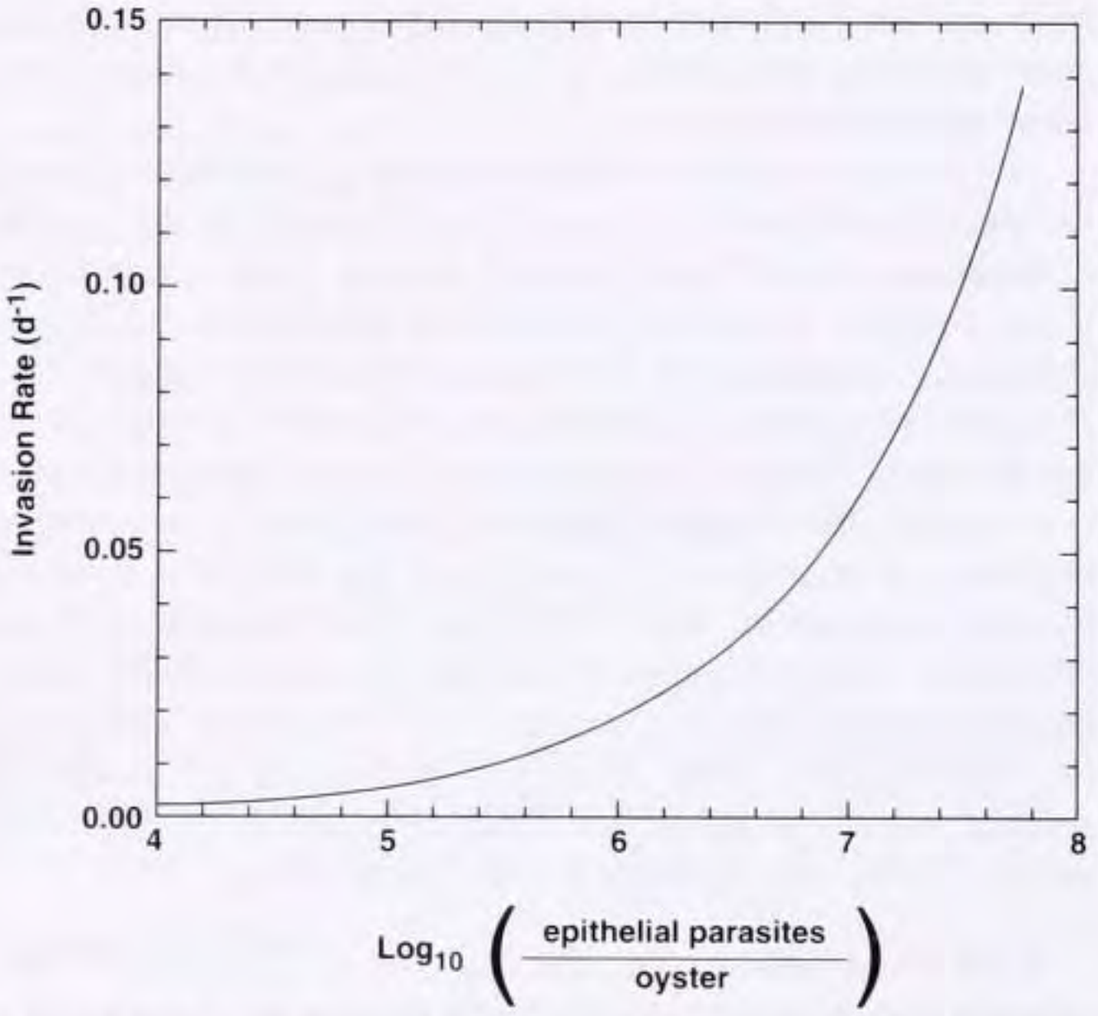

Figure 8. Relationship of the invasion (diffusion) rate of *Haplosporidium nelsoni* from oyster epithelial to systemic tissue and the number of parasites in the epithelial tissue. The rate shown is the one for the initial invasion of parasites into the systemic tissues.

where the values used to determine the rate of decay in susceptibility of *H. nelsoni* cells to hemocytes ($SD_{e/s}$) differ for the epithelium and systemic tissue. Parasites in the epithelium are assumed to recover more rapidly for the same reason that they are less susceptible to the degree-day factor. As long as $\Delta°$ is negative (ambient temperature increasing) the parameter $HSus_{e/s}$ is decreased each time step by *H Decay* amount.

Hemocyte removal of damaged H. nelsoni plasmodia. Once susceptible because of cold-associated damage, *H. nelsoni* plasmodia can be removed by oyster hemocytes at a rate that is dependent on temperature. The hemocytes are assumed to become maximally active at 10 °C and their activity to decrease above 10 °C (Fisher and Tamplin 1988). This is given by an equation of the form:

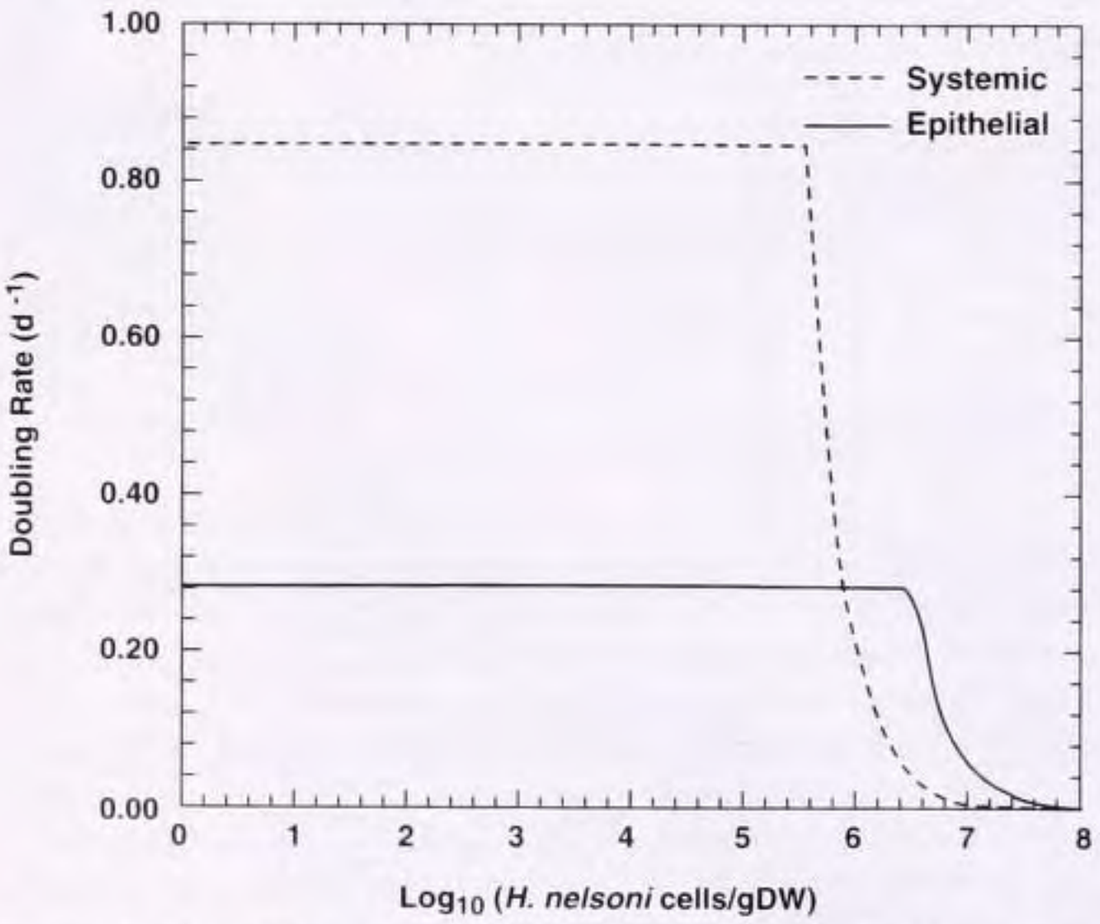

Figure 7. The relationship between the reduction in *Haplosporidium nelsoni* proliferation rates in oyster epithelial and systemic tissue as a function of increasing parasite density (self crowding) at salinities ≥ 15 ppt and a temperature of 20 °C.

$$HR(T) = hr_0 e^{\theta(max(T,10)-Th_0)} \quad (12)$$

where the base hemocyte activity rate, hr_0, is related to the rate at 20 °C (Th_0). The observation that the rate at which oyster hemocytes phagocytose foreign particles is reduced below 10 °C (Feng and Feng 1974, Alvarez et al. 1989) is incorporated into the model as a linear decline to zero in hemocyte activity from 10 °C down to 0 °C.

Net Proliferation of *H. nelsoni*

From the above relationships, the net doubling time of *H. nelsoni* in the epithelial (NG_e) and systemic (NG_s) oyster tissue is given by:

$$NG_e = G_e - HR(T)\, HSus_e\, ehcrowd \quad (13)$$

$$NG_s = G_s - HR(T)\, HSus_s\, crowd_s \quad (14)$$

where the final terms represent parasite density effects on overall hemocyte effectiveness. For systemic infections, this term is the same as that used for parasite crowding effects in equation (5) and accounts for the fact that the increase in circulating hemocyte concentrations stimulated by *H. nelsoni* infection is relatively less than the increase in parasite density (Ford and Kanaley 1988, Ford et al. 1993). Thus, the fraction of the *H. nelsoni* population removed by hemocytes becomes progressively lower as the number of parasites increases.

The value for parasite concentration in the epithelium at which crowding occurs, $crowd_{eh}$, as applied to hemocyte activity, is calculated from equation (5); however, the parasite concentration at which crowding occurs is 17% larger (Table 2) than the constant for epithelial tissue used in equation (5). Once again, this value was established through comparison of simulation results and field observations, because there are no direct observations of this effect. The higher value for the coefficient, $crowd_{eh}$, indicates that hemocytes in the epithelial tissue remain active at proportionally higher *H. nelsoni* numbers than in the systemic tissue. In the ab-

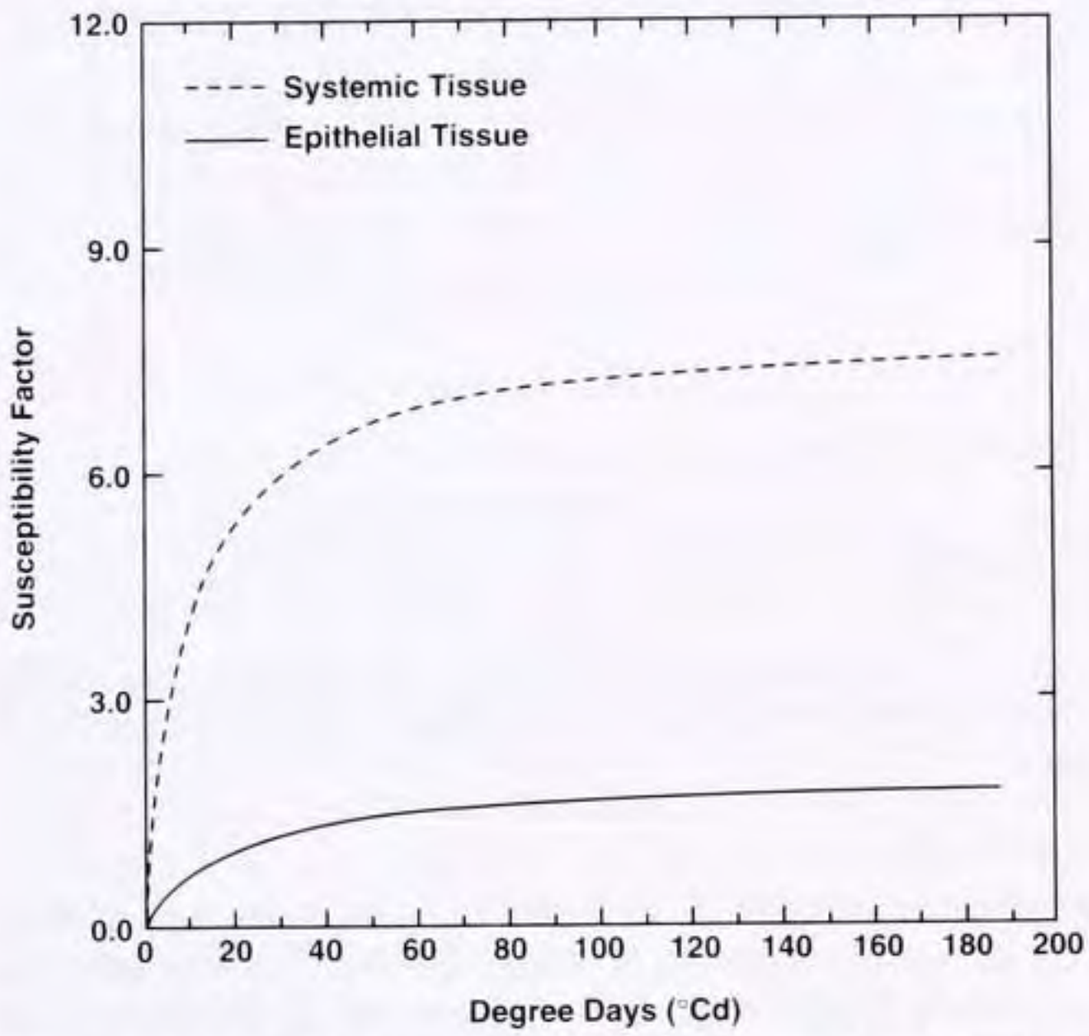

Figure 9. Relationship between the number of degree days below 5 °C and *Haplosporidium nelsoni* susceptibility to destruction by oyster hemocytes in epithelial and systemic tissues.

sence of processes discussed in subsequent sections, equations (13) and (14) determine the values of α and β in equation (2).

H. nelsoni Proliferation in Spring

The increase in *H. nelsoni* infection prevalence and intensity in early spring shortly after the late winter die off (Fig. 1A, point 4), which coincides with rising water temperature, cannot be reproduced in the model through a simple temperature effect on doubling rate. The speed of the increase suggests that density-dependent control on parasite proliferation in the oyster has been released. The biological rationale for this argument is based on observations that, in spring, a rapid increase in oyster growth rate occurs associated with the spring bloom and rising water temperature. For purposes of the model, the environment experienced by *H. nelsoni* inside its host is assumed to improve concurrently as a consequence of an inflow of nutrients, favoring rapid parasite proliferation. It is this fastidious dependency of *H. nelsoni* on nutrients supplied to its host that will dominate the remainder of the post-infection oyster-*H. nelsoni* model.

The effect of changing nutrient supply in the spring was included in the model by relating the density-dependent control on *H. nelsoni* proliferation to food intake by the oyster through filtration and ingestion. In spring, when algal supply and oyster filtration rate are high, the density-dependent control on *H. nelsoni* proliferation is reduced, allowing the parasite to remain in the exponential phase of its growth with maximum cell division rates for a relatively long period. This effect is included in the model through a potential growth efficiency ratio (*NGER*) that is calculated as:

$$NGER = \frac{assimilation - respiration - reproduction}{assimilation} \qquad (15)$$

where oyster *assimilation*, *respiration*, and *reproduction* are calculated using the relationships given in Hofmann et al. (1992, 1994). Equation (15) gives the fraction of net production available to *H. nelsoni* after the oyster's respiratory and reproductive demands have been met, i.e., it is the oyster's potential growth efficiency. The term "potential," rather than "net," growth efficiency is used because some fraction of assimilated energy is utilized by *H. nelsoni*, rather than by the oyster, and this fraction should thus be subtracted from assimilated energy in the calculation of net growth efficiency (e.g., Hofmann et al. 1995, Eq. 1). Potential growth efficiency would be energy available for oyster growth if *H. nelsoni* were not present.

The value of *NGER* from Equation (15) is used to calculate *I factor* in the relationship that determines density-dependent crowding (equation 5) as:

$$Ifactor = max\left[1, \left(\frac{NGER}{NGER_0\, W_0}\right)^{cp}\right] \qquad (16)$$

where $NGER_0$ is the threshold value above which the modified net production (*NGER*) is available to *H. nelsoni*. The threshold value was determined empirically through a series of simulations designed to reproduce the annual cycle of *H. nelsoni* infection and intensity observed in Delaware Bay (Ford and Haskin 1982). The release of the crowding effect occurs only when $NGER \geq 0$. The effect of *I factor* is to increase the number of *H. nelsoni* parasites that must be present before density-dependent controls on parasite proliferation become a regulating factor.

Sporulation of *H. nelsoni*

The factors governing spore production in *H. nelsoni*-infected oysters and the role of spores in its life cycle are among the least understood aspects of this parasite (Haskin and Andrews 1988). The parasites rarely form spores in adult oysters, but may do so regularly in juveniles in both spring and autumn (R. D. Barber et al. 1991, Burreson 1994). Spores can be shed from live oysters, but it is likely that most oysters die during or after sporulation because their infections are so heavy (R. D. Barber et al. 1991). In histological sections of adult oysters with advanced infections at the spring peak, parasites often appear degenerate, with large anomalous nuclei. These abnormal plasmodia may be evidence of a failed attempt at sporulation, after which the parasite dies without completing its life cycle.

For purposes of the model, sporulation or abortive sporulation is hypothesized to be responsible for the rapid disappearance of *H. nelsoni* from oysters in late spring to early summer (Fig. 1A, point 5). In the model, parasites in heavily infected oysters, LFU ≥ 4, can attempt to sporulate, with two possible results. The first is that sporulation is successful, in which case spores are formed and released into the environment. Some oyster mortality is associated with this process. The second possibility is that sporulation is attempted, but is unsuccessful. Failed sporulation makes *H. nelsoni* more susceptible to oyster hemocytes, which remove the parasites and produce oysters with lighter infections. It may also happen that parasites in the heavily infected oysters do not attempt sporulation.

The first part of modeling sporulation required determining whether or not *H. nelsoni* should attempt sporulation; that is, to model conditions within the oyster that would, or would not, favor spore development. The reason or reasons that small oysters support sporulation whereas large oysters typically do not is unknown. The model, however, assumes that it is related to the higher growth efficiency of young oysters, which is reflected in higher *NGER*

values. The approach taken is based on the assumption that sporulation requires a period of good environmental conditions, characterized by high oyster potential growth efficiency, which provides a surplus of required nutrients or other factors to *H. nelsoni* and consequently permits sporulation. Thus, the model accumulates the value of *NGER* from equation 15 ($NGER_d$) over time to obtain a measure of the "internal environmental quality" of the oyster in terms of its ability to support *H. nelsoni* development (Fig. 10, step 1). This was done at each time step such that:

$$NGER_d^{new} = NGER_d^{old} + max\ (NGER - NGER_{d0}, 0)\ \Delta t \quad (17)$$

where Δt is the time step of the model. As *NGER* exceeds the value of $NGER_{d0}$, the quality of the parasite's environment improves and the parasite benefits from the improved conditions, e.g., $NGER_d$ is positive. Equation (17) provides the basis for the remainder of the approach used to simulate sporulation (Fig. 10). Thus, the equations that control sporulation are structured around the seasonal cycle of oyster food availability (Fig. 9).

When $NGER - NGER_{d0}$ is negative, as during periods of low food, $NGER_d$ does not accumulate and sporulation cannot occur (Fig. 10, step 2). However, the time span of high nutrient availability required for sporulation need not be continuous so $NGER_d$ does not decline during periods when nutrient availability is low.

Times when $NGER_d$ is above zero have 4 possible outcomes. The first occurs if a positive $NGER_d$ occurs during times when plasmodia are susceptible to cold (Fig. 10, step 3). It is assumed that cold-damaged plasmodia cannot take advantage of the improving quality of the internal host environment. When the sum of the cold-exposure death rates of *H. nelsoni* in the epithelial and systemic tissue (equations 10 and 12) exceeds 0.1 d^{-1}, $NGER_d$ is not accumulated.

The second and third possible outcomes occur when the *H. nelsoni* plasmodia are healthy and the internal quality of the host is improving (e.g., $NGER_d$ is positive). At these times, sporulation

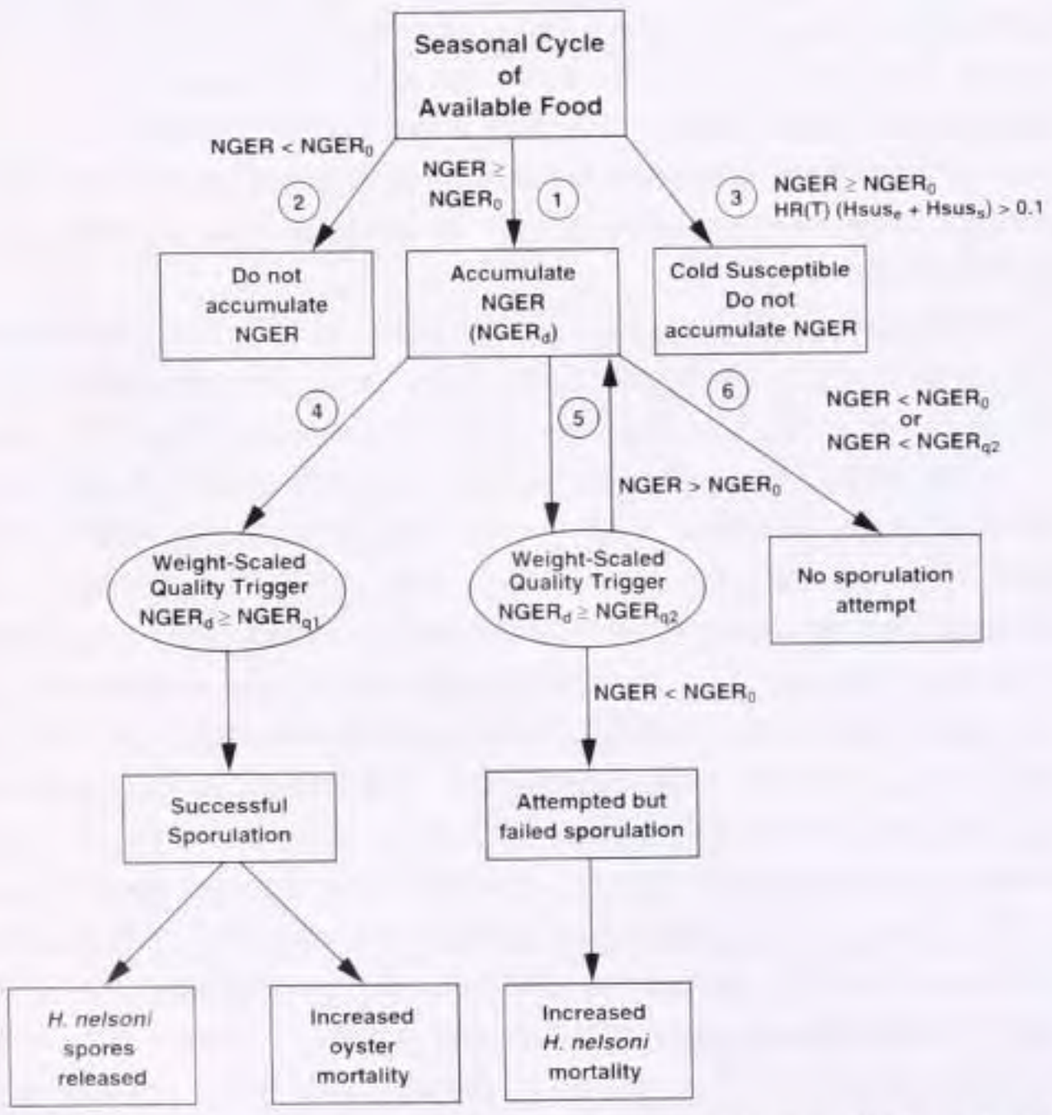

Figure 10. Schematic showing the potential pathways that may arise during sporulation and attempted sporulation by *H. nelsoni*. The numbers correspond to specific sporulation processes that are described in the text.

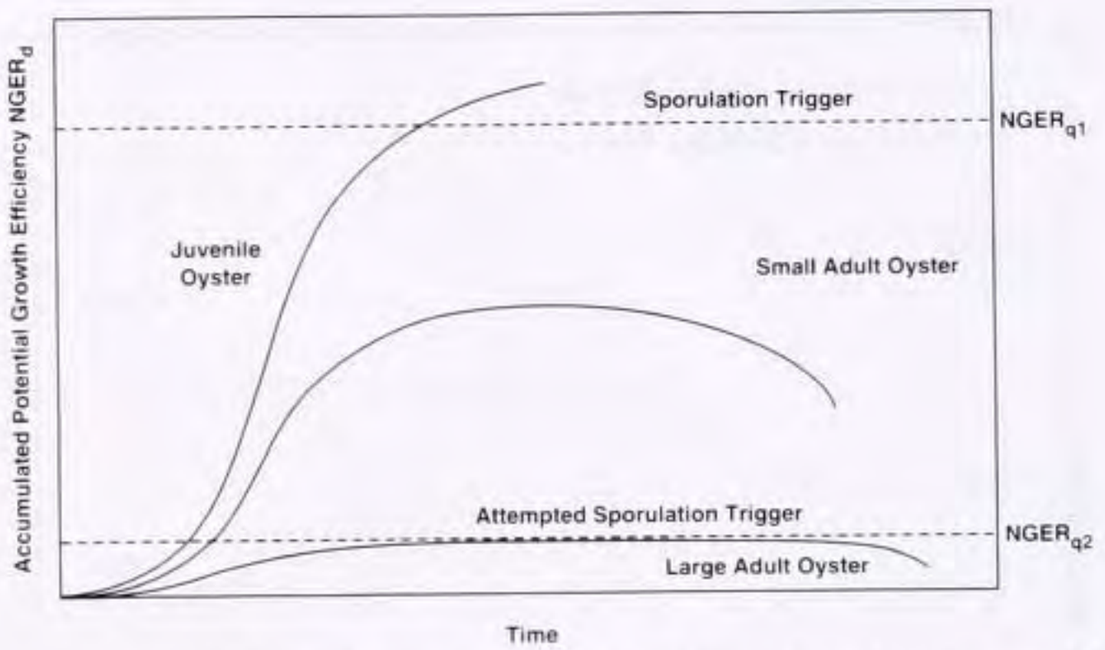

Figure 11. Relationship between $NGER_d$, the accumulated potential growth efficiency ratio, and the sporulation triggers for oysters of 3 sizes.

becomes a possibility. It is assumed that, as $NGER_d$ is accumulating and the oyster quality is becoming more favorable, parasites are cued to begin the sporulation process. In the second possible outcome, sporulation is successful. For successful completion of this process, a certain level of internal host quality must be attained (Fig. 10, step 4). The quality trigger ($NGER_{q1}$) for sporulation was set at 100 $gdwt^{-1}$, a value determined empirically through the comparison of a series of simulations and field observations. As noted above, sporulation success is related to the size of the oyster host, with successful sporulation predominating in small oysters. Thus, the quality trigger is scaled by the size of the host and, when $NGER_d$ exceeds the quality threshold ($NGER_d \geq NGER_{q1}\ W_0$), sporulation is triggered and $NGER_d$ is reset to zero (Fig. 11). The value of 100 $gdwt^{-1}$ permits sporulation in small (up to about 2 cm in length) oysters because of their higher potential growth efficiency, but does not permit sporulation in larger oysters.

In the third possible outcome, sporulation is unsuccessful. In larger oysters, quality also improves as $NGER_d$ accumulates, but because of lower potential growth efficiency and, consequently, fewer resources available to the parasite, the sporulation trigger is rarely reached. In these oysters, the parasites prepare for sporulation, but the spring bloom ceases and nutrient levels decline before enough nutrients are obtained to sustain sporulation. When nutrient levels decline enough that $NGER - NGER_{d0}$ becomes negative, abortive sporulation occurs in animals that have accumulated $NGER_d$ above a second weight-scaled quality trigger ($NGER_{q2}$ = 10 $gdwt^{-1}$): $NGER_d \geq NGER_{q2}\ W_0$ (Fig. 10, step 5). When this happens, $NGER_d$ is reset to zero.

It is also possible that the accumulated value of $NGER_d$ will not exceed either quality trigger ($NGER_{q1}$, $NGER_{q2}$). In this fourth possible outcome, sporulation is not attempted and infection intensity continues to increase as determined by the parasite doubling time (Fig. 10, step 6).

Sporulation and attempted sporulation do not occur instantaneously in all oysters meeting the nutritive requirements for the process. The rate of sporulation or attempted sporulation (*SporeS*) is high immediately after the conditions of the nutritive triggers are met and decays over time. The base rate, *SporeS*, is defined as 0.1 LFU, which produces the desired result that sporulation and attempted sporulation events occur more frequently at higher infection intensities. This rate decreases linearly over time by first setting $SporeS_d = 1$, and then establishing a rate of decay.

$$SporeS_d^{new} = SporeS_d^{old}\ (1 - \Delta t SSR) \quad (18)$$

where *SSR* sets the decay rate such that sporulation or attempted sporulation ceases 60 days following the initial trigger. Sixty days provides simulations that best fit field observations of *H. nelsoni* infection intensity during the summer sporulation event. In any given time step, then, the number of oysters undergoing sporulation or attempted sporulation is:

$$O^{p}_{e,s} = SporeS\ SporeS_{d}\ O_{e,s} \tag{19}$$

where $O^{p}_{e,s}$ are those oysters undergoing sporulation or attempted sporulation.

Spores are formed at times of rapid parasite proliferation, in the spring and late summer/early fall (R. D. Barber et al. 1991, Burreson 1994), but the marked decline in prevalence and intensity that is hypothesized to occur, at least partly as a result of failed sporulation (i.e., incomplete life cycle), occurs only in the spring as water temperatures exceed about 20 °C (Andrews 1966, Ford and Haskin 1982). This observation suggests an influence of temperature on sporulation and attempted sporulation such that neither process occurs at temperatures where *H. nelsoni* is cold susceptible and the process occurs at fastest rates above 20 °C despite adequate nutritive values ($NGER_{d}$). Therefore, a temperature-dependent "spore susceptibility" factor (*TempSS*) was used to modify equation (19). The temperature factor was defined as:

$$TempSS = \Delta t \frac{1 + tanh\left(\frac{T - SST_{0}}{SST_{sp}}\right)}{2} \tag{20}$$

which allows sporulation to be set in motion at about 9 to 10 °C and reach a maximum rate at 21 °C (Fig. 12). The coefficients, SST_{0} and SST_{sp} determine the temperature at which *TempSS* is one-half its maximum rate and the temperature range over which the spore susceptibility switches from little to maximum effect (Fig. 12). The temperature effect modifies equation (19) as:

$$O^{p}_{e,s} = TempSS\ SporeS\ Spore_{d}\ O_{e,s} \tag{21}$$

Failed sporulation results in death of *H. nelsoni,* their removal by hemocytes, and a lower intensity infection in the oyster. One-half of the oysters assumed to lose all parasites due to failed sporulation are placed in the uninfected oyster class ([0,0], equation 3). The remaining one-half are placed into the lowest epithelial, no-systemic infection ([1,0], equation 2) class.

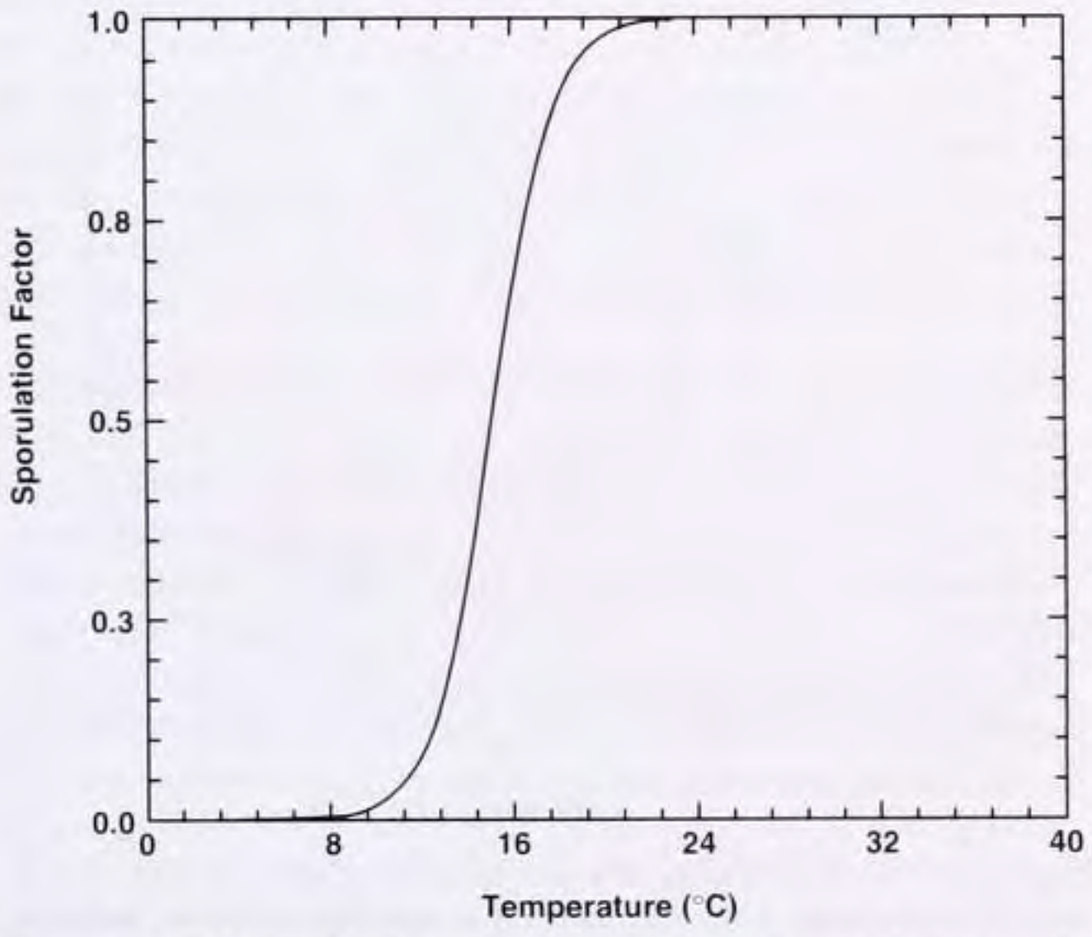

Figure 12. Relationship between the rate at which sporulation can be attempted and temperature.

Successful sporulation occurs during periods when the quality of the host's internal environment increases to the point that the weight-scaled sporulation trigger ($NGER_{q1}$) is exceeded (Fig. 11). The factors that determine the number of oysters in which successful sporulation occurs are similar to those that affect the number of oysters undergoing failed sporulation, with the exception that some oyster mortality also occurs in the process. Therefore, equation (21) is used to calculate the number of oysters surviving sporulation. Successful sporulation results in the death of some fraction of the affected oysters. The number of oysters with infections in systemic LFU category 4 and all epithelial categories that die from the sporulation event is calculated as:

$$O^{d}_{e,s} = Spore_{k}\ SporeS\ O_{e,s} \tag{22}$$

where the initial rate at which oysters die as a result of sporulation ($Spore_{k}$) is assumed to be equivalent to a four-day halving time. The dead oysters are removed from subsequent calculations.

Successful sporulation releases *H. nelsoni* spores into the environment. The total number of spores released (*TotalS*) can be calculated as:

$$TotalS = O_{e,s}\ SpFrac\ SporeN\ (frac_{e}\ cells_{e} + frac_{s}\ cells_{s}) \tag{23}$$

where *SpFrac* is the fraction of the parasites that undergo successful sporulation and *SporeN* is the number of spores formed by each *H. nelsoni* plasmodium (Table 2).

Salinity Effects on *H. nelsoni*

Laboratory (Sprague et al. 1969, Ford and Haskin 1988) and field observations (Farley 1975, Haskin and Ford 1982, Andrews 1983, Ford 1985b) have shown salinity to be a critical environmental factor regulating the spatial and temporal distribution of *H. nelsoni* in oyster populations. The following paper (Paraso et al. this volume) describes many of these interactions and provides detailed descriptions of how the coupled model simulates salinity-*H. nelsoni* interactions. However, a brief accounting of these parameterizations is given here for completeness in the model description. In the model, salinity affects *H. nelsoni*-oyster interactions by controlling parasite proliferation rate, mortality rate, transfer rate from epithelial into systemic tissues, and infection rate.

The basis for the effect of salinity on *H. nelsoni* proliferation *in vivo* is a relationship derived from measurements of acute *in vitro* salinity tolerance of the plasmodial stage of *H. nelsoni* (Ford and Haskin, 1988). This relationship shows that, at a salinity of less than 5 ppt, *H. nelsoni* survival is zero. Between 5 and 15 ppt, the parasites show an exponential increase in survival, and above 15 ppt little mortality occurs (see Paraso et al. this volume, Fig. 3). The salinity-caused mortality (*Smort*) was modeled as:

$$Smort = min\left(1, \frac{0.01\ SD_{1}}{1 + \frac{SD_{1} - SD_{2}}{SD_{2}} e^{-SD_{3}S}}\right) \tag{24}$$

where S is the ambient salinity in ppt and SD^{1}, SD^{2}, and SD^{3} are constants. The actual salinity-induced parasite death rate is calculated as:

$$Sdeath = \frac{-ln(Smort)}{SD_{4}} \tag{25}$$

where the death rate calculated from *in vitro* data is assumed to occur over four days (SD_4) to account for the buffering effect of an *in vivo* situation (Galtsoff 1964, Shumway 1996). The salinity-caused mortality modifies the net proliferation rates in the epithelial and systemic tissues that are given by equations (7) and (8). Unlike other sources of mortality, salinity-caused mortality is assumed to be able to completely eliminate infections. This occurs at mortality rates above 0.01787 d^{-1}.

It was assumed that salinity effects on parasite proliferation rates would occur over the same salinity range as that producing parasite mortality; hence, the effect of salinities between 5 and 15 ppt on parasite doubling time was included through an exponential relationship:

$$Sfactor = e^{sg(S-S_0)} \tag{26}$$

that varied between zero ($S \leq 5$ ppt) and 1 ($S > S_0$), where sg determines the rate of decrease of parasite proliferation rate with increasing salinity and S_0 is 15 ppt, the salinity threshold above which no reduction in parasite proliferation rate occurs. Equation (26) modifies the temperature-dependent growth rate given in equation (4).

In the initial simulations, the frequency of systemic infection decreased with decreasing salinity. Long-term observations in Delaware Bay, however, show that, after an initial decrease from the high salinity (20–23 ppt) planting grounds to the lower-most seed beds (18 ppt), the frequency of systemic infections remains unchanged along the remainder of the salinity gradient to the upper-most seed bed (9 ppt). To simulate the observed pattern, the model increases the rate of parasite diffusion between epithelial and systemic tissue with decreasing salinity by including an additional term of the form:

$$Sdiff = 1 + SF1 \frac{\left\{1 - tanh\left[SF2\left(\frac{S - S_0}{SF3}\right)\right]\right\}}{2} \tag{27}$$

to equation (6). This relationship allows the rate of diffusion between epithelial and systemic tissues to be maximum for salinities of 12 ppt and less, and to decrease to the base rate given by equation (6) between 12 and 18 ppt. It is presently unclear whether the biological basis of the field observations is actually tied to more rapid transfer of parasites, or whether some other mechanism is responsible. Thus, equation (14) can now be updated to its final form:

$$NG_s = G_s - HR(T)\, HSus_s\, crowd_s - Sdeath + diffusion\ Sdiff. \tag{28}$$

Oyster Mortality

The ultimate result of most *H. nelsoni* infections is the death of the oyster host. To model this effect, historical data on the intensity of infection (LFUs) in live and dead oysters was assembled. The percent of live and dead oysters in each infection category was calculated as a function of the total number of live or dead oysters, respectively, in the set of samples examined. The ratio of percent dead to percent live in each category was then computed. This ratio was considered a relative measure of the likelihood that an oyster will die with a given category of infection. Results showed that oysters in LFU categories 1 and 2 are no more likely to die than those in category 0; in categories 3–5, the likelihood rises to between two and three; and oysters with category 6 infections are six times more likely to die than those without detectable infections. This relationship (Fig. 13) is of the form:

$$MortO = \frac{-ln(1 - M_a\, e^{M_b LFU})}{M_{span}}. \tag{29}$$

Abundant field observations show that infected oysters can survive better at low temperatures than at high (Andrews 1968, Ford and Haskin 1982). For instance, as temperatures approach 7 °C in late November in Delaware Bay, the mortality rate drops to nearly zero. It is assumed that this happens because both host and parasite are quiescent at low temperature: the parasite no longer actively damaging the host and the host no longer actively feeling the effects of parasitism. It is a system "on hold" over the winter. Thus, a temperature effect was applied to the death rate given by equation (27) such that oyster mortality is reduced in a linear manner from the rate at 7 °C to zero at 0 °C.

The total number of dead oysters in any infection class is then calculated as:

$$O^d_{e,s} = Spore_k\, SporeS\, MortO\, O_{e,s} \tag{30}$$

which is a modification of equation (22). In addition, any oyster in which the infection intensity exceeds that found in live oysters automatically is placed in the dead oyster category (Fig. 4). The dead oysters are removed from subsequent calculations of infection dynamics, but they are accumulated over time to provide an estimate of mortality.

***H. nelsoni* Transmission**

Transmission is dealt with fully in the third paper in this series (Powell et al. this volume). A condensed accounting of the parameterizations used for this process is given here for completeness in the model description.

The processes by which *H. nelsoni* is transmitted to uninfected oysters, and the form of the infective particle, are not known. However, observations that the earliest infections are in the gill

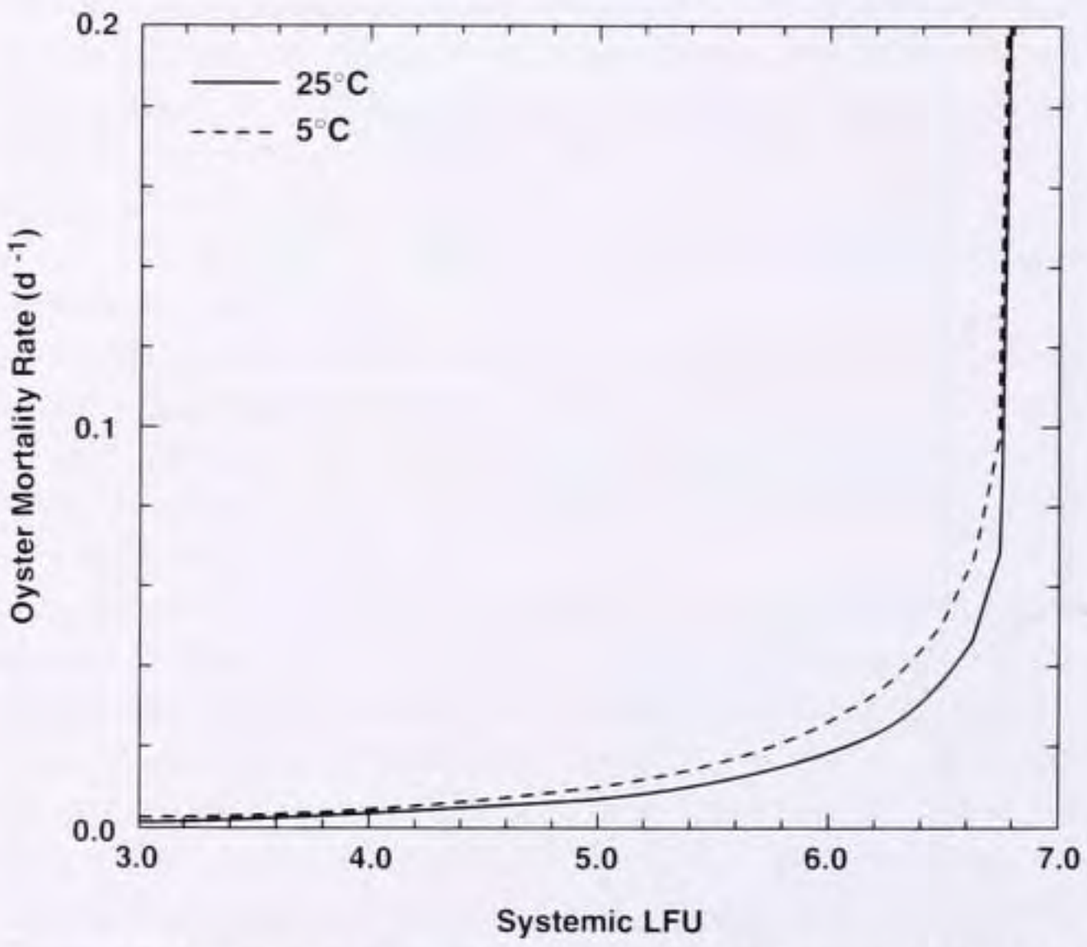

Figure 13. Oyster mortality rate as a function of systemic LFU at 5 °C and 25 °C, which span the range of temperature that is normally encountered in Delaware Bay.

epithelium indicate that infective particles are acquired through filtration (Farley 1968, Ford and Haskin 1982). In addition, early studies with timed imports of oysters into enzootic regions of Delaware and Chesapeake Bays clearly showed that oysters became infected only during a period from late May through early October (Andrews 1968, Ford and Haskin 1982), suggesting that there is a seasonal dependence in the ambient concentration of *H. nelsoni.* The abundance of infective particles in the water is a critical element in modeling transmission, but no measurements are available to parameterize this process. Recently, however, Barber and Ford (1992) reported finding haplosporidian spores, morphologically similar to those of *H. nelsoni,* in the digestive tract lumina of oysters in Delaware Bay and other regions enzootic for *H. nelsoni.* The spores, obviously ingested while feeding, predominated from May through October, the known infective period for *H. nelsoni.* These may not be *H. nelsoni* spores, and if they are, they may not be the stage that infects oysters. Nevertheless, these data are the only ones available on which to base a rough estimate of likely seasonal fluctuations in ambient concentrations of *H. nelsoni* infective particles. Further, both simulations and observations suggested that salinity and temperature, in addition to time of year, affect the abundance of infective particles (see below).

The actual rate at which new *H. nelsoni* infections occur in uninfected oysters (O_{00}) is dependent upon the number of infective particles filtered out of the water. This rate ($\beta_{0,0}$) is given by:

$$\beta_{00} = \frac{I_1}{1 + \frac{I_1 - I_2}{I_2} e^{I_3\, IP\ filter}} \tag{31}$$

where *IP filter* is the number of infective particles filtered by the oyster. The relationship assumes a threshold dose of 8,700 infective particles filtered d^{-1} needed to generate a new infection. The rationale for using this value is given in Powell et al. (this volume). The remainder of the transmission submodel is designed to estimate *IP filter.*

The number of infective particles filtered by the oyster was modeled as:

$$IP\ filter = IPConc\ filt(size)\ IPseason\ IPsal\ IPtemp \tag{32}$$

where *IPconc* is the ambient infective particle concentration in the water column, *filt(size)* is oyster filtration rate, *IPtemp* and *IPsal* are the temperature and salinity effects on infective particle abundance, respectively, and *IPseason* is the seasonal variation in infective particle availability. Oyster filtration rate is calculated using the relationships given in Hofmann et al. (1992, 1994). The relationships used to specify the seasonal, salinity and temperature dependencies of the infective particles are described below.

Seasonal effects. The base concentration of infective particles, IP_{conc}, was chosen by comparing results of simulations using a range of values to field observations of prevalence (discussed in Powell et al. this volume). The base concentration was then modified seasonally based on observations of ingested haplosporidian spores, which revealed that spores were present primarily during the May–October period (Barber and Ford 1992). This time series (Fig. 14) was taken to reflect the relative abundance of infective particles and was included in equation (32) as *IPseason.*

Local salinity effects. Initial simulations of *H. nelsoni* prevalence in low-salinity oysters showed that prevalences were higher than those observed and suggested that the rate of infection, as well as the rate of proliferation within oysters, decreases with decreasing salinity (Paraso et al. this volume). A function that decreased the concentration of infective particles in low salinity water resulted in simulated prevalence levels and patterns that better match those recorded on the low-salinity Delaware Bay seed beds (Paraso et al. this volume). The function was obtained by using the model to simulate infections over a broad range of salinities in Delaware Bay and comparing these to long-term time series (Haskin and Ford 1982, Fegley et al. 1994). Based on these comparisons, the effect of local salinity on transmission rate was modeled as:

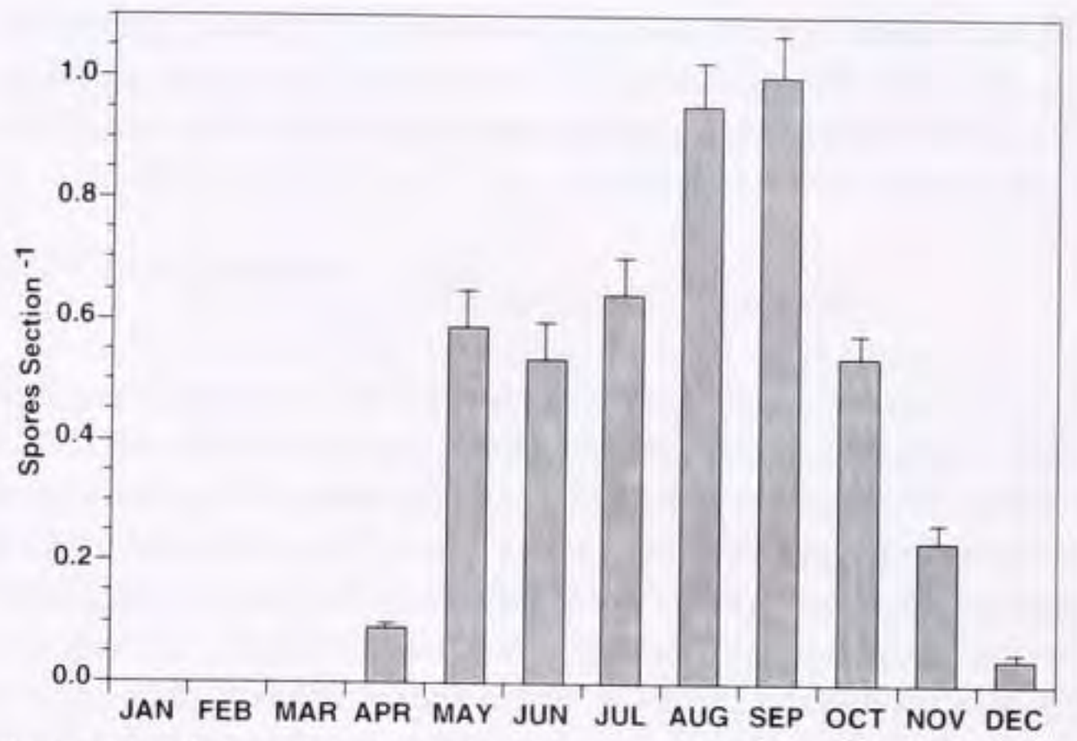

Figure 14. Time series of putative *Haplosporodium nelsoni* spores observed in sectioned *Crassostrea virginica* gut lumena as described in Barber and Ford (1992).

$$IPsal = \frac{1 + tanh\left(SM_1 \frac{(S - SM_0)}{SM_2}\right)}{2}. \tag{33}$$

The relationship makes biological sense because the salinity range affecting transmission is similar to the range affecting parasite mortality in the host and the somewhat wider range is anticipated for a potentially free-living infective particle. Whether the model simulates decreased survival of infective particles, their decreased ability to infect, or simply a dilution factor, is unknown.

Bay-wide oscillations. Simulations with long-term time series that were designed to test the adequacy of the transmission submodel, using the basic process of oyster filtration, infective dose, the seasonal cycle of infective particle availability, and a local effect of salinity on infectivity, showed adequate simulations for oyster populations over a wide salinity range in a specific bay, such as Delaware Bay (e.g., Paraso et al. this volume), during most years. However, the same parameterizations failed in Chesapeake Bay. Although the seasonal cycle of infective particle availability may be somewhat different, certainly the remaining processes should be equivalent in both bays. This suggested that an additional process was needed to model transmission rate.

Review of long-term time series taken simultaneously at multiple sites across the salinity gradient in both bays revealed relatively simultaneous oscillations in disease prevalence with salinity change. Addition of bay-wide salinity-dependent multi-year oscillations in infective particle availability allowed both bays to be modeled with very minor differences in the values of only 2 vari-

ables, $IPconc_0$ and $IPconc_{max}$. (Variations in $IPconc_{max}$ are discussed in the third paper in this series, Powell et al. this volume). These oscillations were parameterized as follows. The rate of salinity change was calculated as:

$$IPsalrate = IPsalrate_0 \left(\frac{S_{IP} - IPsal_0}{IPsal_1} \right) \quad (34)$$

where $IPsalrate_0$ specifies the response time of the infective particles to changes in salinity, which was taken to be 180 days. The salinity value used to specify S_{IP} can be considered representative of the salinity at which an hypothetical *H. nelsoni* secondary host lives or where some other reservoir of infective particles is found. For the simulations given in the following sections, the value of S_{IP} was taken from the most down estuary (highest salinity) site showing strong salinity excursions across the 15 ppt isohaline in both Delaware and Chesapeake Bays. Lower salinity sites failed to provide adequate simulations in either bay, as discussed in Powell et al. (this volume) and higher salinity sites were not present in the suite of available Chesapeake Bay time series. The concentration of infective particles was updated at each time step based on this rate (*IPsalrate*) forced by the direction and migration of salinity change. So, for increasing salinities ($IPsalrate \geq 0$),

$$\frac{dIPconc}{dt} = IPsalrate(IPconc_{max} - IPconc). \quad (35)$$

For decreasing salinities (IPsalrate < 0),

$$\frac{dIPconc}{dt} = IPsalrate(IPconc - IPconc_{min}) \quad (36)$$

and, at model initialization, $IPconc = IPconc_0$. The new value of *IPconc* was then inserted into equation (32).

Temperature effects. Long-term observations from Delaware Bay show a cyclic pattern of *H. nelsoni* activity in which years of low infection prevalence follow, typically with a lag of 1 to 2 years, very cold winters (Ford and Haskin 1982). Examination of a 1989 to 1994 data set for Chesapeake Bay showed the same phenomenon. Thus, in some years, very few oysters become infected, even when appropriate salinity conditions are present (Haskin and Ford 1982, Paraso et al. this volume). This pattern suggests that, in some way, the abundance of infective particles is diminished after cold winters.

In the model, direct temperature effects on infective particle abundance were included through a calculation of degree days that is based on 10 °C (*DD*10). This calculation differs from that for cold susceptibility (equation 9), which considers temperature effects on *H. nelsoni* after it has infected the oyster.

The number of days in which the temperature is below 10 °C from January to May is accumulated as:

$$DD10 = \sum_{t=1JD}^{t=150JD} 10 - T \quad (37)$$

where JD refers to Julian days. The value of *DD*10 is then used to determine an estimated degree to which cold temperature affects the survival of infective particles as:

$$IPtemp_{est} = \frac{1}{2} \left\{ 1 - tanh \left[DD_2 \left(\frac{DD10 - DD_0}{DD_1} \right) \right] \right\} \quad (38)$$

where DD_0 is a threshold value at which the temperature effect becomes active.

Equation (38) provides a value for the temperature effect that is based on the current degree-day calculation. To model the observed delay in the manifestation of winter temperature effects on *H. nelsoni* infective particles, the value of *IPtemp* determined from the current *DD*10 value was modified based on the value calculated for the previous year. A current value of *DD*10 less than one-half of the threshold value (DD_0), indicates that the current year's winter is considerably warmer (an extreme difference) than that in the previous year, and the current value of $IPtemp_{est}$ is used as *IPtemp*. If the current value of *DD*10 is greater than one-half DD_0 and less than the value for the previous year, such that the current year's winter is only slightly warmer than the previous year's winter, the current and previous year's values are averaged to obtain the value for *IPtemp*. This allows the conditions in the previous winter to affect the level of infectivity by *H. nelsoni* and thereby allows for persistence of the effects of harsh winters over a period of more than 1 year, as observed. If *DD*10 is greater than one-half DD_0 and greater than the value calculated for the previous year, then the current conditions are colder than previous year's conditions and also characteristic of a cold winter. In this case, *IPtemp* is specified using the current value of $IPtemp_{est}$.

Data Sets

Environmental Time Series

The environmental inputs to the oyster population-*H. nelsoni* model are time series of temperature, salinity, food, and total seston (total suspended solids). The time series used for simulations presented in the next section are characteristic of the environmental conditions on the lower Delaware Bay planted grounds (Fig. 1 in Paraso et al. this volume). These reference simulations are intended to reproduce the annual *H. nelsoni* cycle in high salinity.

Temperature measurements were made at a representative site, Miah Maull, by personnel from the Haskin Shellfish Research Laboratory at intervals of 1 to 3 measurements per month throughout the decade of the 1960s. These data show that the winter of 1962 and those from 1968 to 1970 were particularly cold (Fig. 3a in Powell et al. this volume). Salinity time series for the 1964 to 1968 period were derived from monthly-averaged Delaware River flow measurements taken at Trenton, New Jersey, by the U.S. Geological Survey. Salinity time series were calculated using the relationship between Delaware River flow and salinity derived by Haskin (1972) as described in Paraso et al. (this volume). This relationship accurately represents salinity conditions during the 1960s in Delaware Bay, but may be less representative of salinities thereafter because of changing river flow to salinity relationships in the estuary (Haskin 1972). The 1960s were characterized by increasingly saline conditions in the first 6 years of the decade (Fig. 4 in Powell et al. this volume), followed by a freshening trend that began in 1967. The saline conditions in 1963 to 1967 coincided with a period of average-to-relatively mild winters. The salinity during this time was optimal for the proliferation and spread of *H. nelsoni*. The intent of the oyster-*H. nelsoni* model is to simulate the basic cycle observed for *H. nelsoni* prevalence and intensity. By using the time series for 1964 to 1968, the simulations were not influenced by anomalous environmental conditions that would limit *H. nelsoni* proliferation.

Measurements of food and total seston at the Miah Maull site are not available for any time during the 1960s; however, total seston and chlorophyll measurements were made at other lower-estuary locations in Delaware Bay by Haskin Shellfish Research

Laboratory (HSRL) scientists at about monthly intervals from 1981 to 1986, with the sampling frequency increased to bi-weekly between 1982 and 1984. The chlorophyll and total seston time series given by Powell et al. (1997) were used in the reference simulations. Measurements made at a site just south of Egg Island, New Jersey, were assumed to be representative of the Miah Maull planting grounds (Fig. 1 in Paraso et al. this volume). The 6-year time series from this site was averaged to obtain a single time series of 1-year duration that was used for each year of the simulations.

Total suspended solids at the site showed variability throughout the year, with maximum values tending to occur in late spring to early autumn (Fig. 6 in Powell et al. this volume). The chlorophyll time series shows a distinctive spring bloom that occurs in March to May, with the maximum in March (Fig. 6 in Powell et al. this volume). A consistent fall bloom does not occur, although transient increases in chlorophyll concentration do occur from time to time. Chlorophyll values drop to seasonally low levels in July and remain, for the most part, at or near these levels until the next spring. Chlorophyll *a* in $\mu g\ L^{-1}$ was converted to oyster food in mg DW L^{-1} using the relationship derived by Powell et al. (1997) from Soniat et al. (1998):

$$food = \alpha \times chlorophyll\ a + \beta \qquad (39)$$

where $\alpha = 0.088$ mgdw $(\mu g\ chl)^{-1}$ and $\beta = 0.26$ mgdw L^{-1}.

H. nelsoni Prevalence and Intensity Time Series

H. nelsoni prevalence and intensity were measured at numerous sites in Delaware Bay from 1959 to 1992 by personnel from the Haskin Shellfish Research Laboratory (Ford and Haskin 1982, Haskin and Ford 1982, Fegley et al. 1994). These measurements (Fig. 1A) provide the calibration and verification for the reference simulation (described in the next section) obtained from the oyster-*H. nelsoni* model for lower Delaware Bay.

Model Implementation

The oyster-*H. nelsoni* model was solved numerically using a 2-step pseudo-steady state approximation scheme (Verwer and van Loon 1994) with a time step of 1 hour. Each simulation begins on 1 June 1964 and extends through December 1968. The first simulation established a reference to which all other simulations were compared. The reference simulation was designed to reproduce the seasonal cycle of *H. nelsoni* prevalence and intensity as observed in a high-salinity location (Fig. 1A). Subsequent simulations were designed to show the modifications to this seasonal cycle that arise when some of the assumptions used in developing the oyster-*H. nelsoni* model were relaxed or removed (Table 4). In this regard, these simulations serve as a measure of the sensitivity of the model to the assumptions on which the model is based. Other simulations evaluate the response of the model to variations in environmental conditions.

RESULTS

Reference Simulation

The simulated time-development of *H. nelsoni* infection in oysters from June 1964 to December 1968 (Fig. 15a), using the environmental time series from the Miah Maull site in Delaware Bay, reproduces the observed annual cycle (Fig. 1A). The first (June 1964 to June 1965) and third (June 1966 to June 1967) years show

TABLE 4.

Simulations done with the oyster-*H. nelsoni* model to test the effect of certain model assumptions and environmental conditions on the simulated infection prevalence and intensity. For each simulation, the changes made in the environmental conditions, oyster size, or model dynamics relative to the conditions used to produce the reference simulation are given. The figure number showing the resultant simulation is indicated.

Simulation	Environmental data set	Oyster size (g)	Model change	Figure number
Reference	Miah Maull 1964–1968	1	none	15a
Crowding effect	Miah Maull 1964–1968	1	density-dependence effect removed (equation 5)	15b
Winter temperature	Miah Maull 1964–1968	1	cold suscep. of *H. nelsoni* removed (equation 10)	15c
Food effect on sporulation	decreased food in 1965	1	none	16a
Spring food effect	no spring bloom in each year	1	none	16b
Oyster size-sporulation effect	Miah Maull 1964–1968	0.3	none	17a
Oyster size-sporulation effect	Miah Maull 1964–1968	0.1	none	17b
Winter temp-sporulation effect	Miah Maull 1964–1968	0.1	winter temperature effect on sporulation removed (equation 20)	18
Cold winter	winter 1965–1966 colder	1	none	19a
Warm winter	winter 1965–1966 warmer	1	none	19b

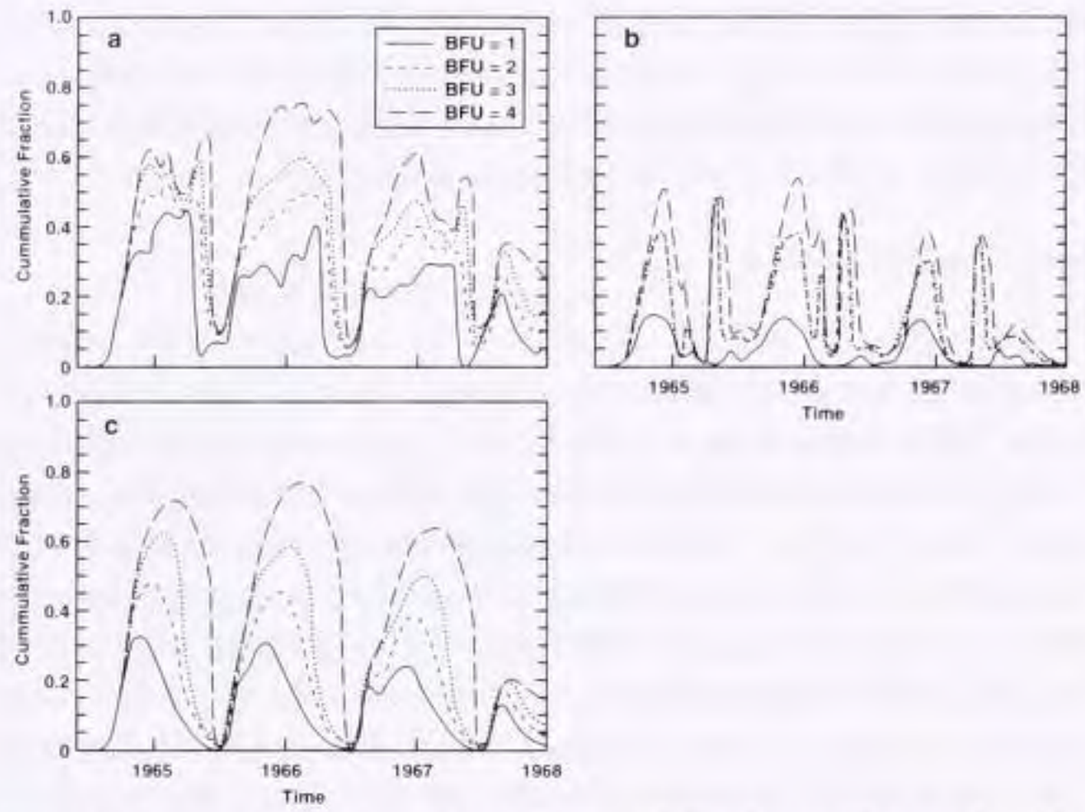

Figure 15. Simulated time-development of *Haplosporidium nelsoni* infection for 1-g AFDW oysters in Delaware Bay using a) the environmental time series from June 1964 to June 1968, which represents the high-salinity, lower Bay grounds; b) with the density-dependent control on *Haplosporidium nelsoni* growth, equation (5), removed; and c) with the cold susceptibility of *Haplosporidium nelsoni*, equation (10), removed. The term "cumulative fraction" means that the line for each BFU category represents the total prevalence of infections in that and all lower categories.

the expected pattern in disease progression, with an increase in June to early fall (Fig. 1A, point 1), a plateauing in fall (Fig. 1A, point 2), the winter decrease (Fig. 1A, point 3), an increase the following spring (Fig. 1A, point 4), and the decrease in late spring (Fig. 1A, point 5). Year 2 has a slightly modified version of this cycle, with the pattern during the late winter being less distinct. Year 4 of the simulation (Fig. 15a) shows the expected progression for the half year that is depicted. The simulated *H. nelsoni* infections are initially primarily epithelial (BFU = 1) and progress rapidly to higher infection intensities. In the first and third years, about 30% to 40% of the oyster population has systemic infections of BFU $\geq$ 2 by late summer. In the second year, over 50% of the oyster population is infected at this level. These year-to-year differences in prevalence result from the different environmental conditions in each year, as discussed in Powell et al. (this volume). The maximum total prevalences of about 60% to 80% that are attained in the early fall agree with the maximum prevalences reported for lower Delaware Bay at this time (Ford and Haskin 1982). Also, the partitioning of the disease between epithelial and systemic infections in the observed and simulated distributions is similar, with about 60% to 70% of the infections being systemic at peak prevalences (Fig. 1A). Thus, the simulated annual cycle of prevalence and intensity accurately reproduces both observed patterns and infection levels.

Sensitivity of Density-Dependence and Cold Susceptibility Factors

One of the assumptions made in the oyster-*H. nelsoni* model is that the plateau in disease intensity in late summer is due to self crowding by the parasites. However, since there is no direct observation of this effect, it is instructive to determine how sensitive the model is to this assumption. To do this, equation (5) was set to zero. Without the density-dependent control, *H. nelsoni* proliferates rapidly in the summer and triggers a large oyster mortality in December and January, sharply reducing prevalence by midwinter (Fig. 15b). Neither mortality nor a drop in prevalence is observed at this time in the field (Fig. 1B). Even without the density dependent control, proliferation of *H. nelsoni* does slow in winter due to the cold temperatures, however, this reduction is not sufficient to limit oyster mortality. In particular, a second large oyster mortality event occurs in the late spring of the second, third, and fourth years of the simulation due to the very rapid increase in *H. nelsoni* cell number as temperatures increase in spring. The excessive mortalities of heavily infected oysters cause the simulated infection levels in surviving oysters to be lower than either the reference or observed values. Observed oyster mortality due to *H. nelsoni* does occur in late spring (Fig. 1B), but it is only 10% to 15% of the oyster population rather than the nearly 50% that die in this simulation.

Similarly, the removal of the cold susceptibility of *H. nelsoni* (equation 10) results in simulated disease prevalences and intensities (Fig. 15c) that do not reproduce the observed annual cycle. In the observed cycle (Fig. 1A) and the reference simulation (Fig. 15a), decrease in *H. nelsoni* prevalence and intensity does not occur in late winter. Removal of cold susceptibility predicts that the high parasite values that were present at the end of the previous summer and fall persist through the next spring. Increasing temperatures and subsequent rapid parasite proliferation result in infection prevalences (almost 80%) and intensities (nearly 80% systemic) that are higher than observed in late spring. These high disease levels are followed by a very large sporulation event and coincident oyster mortality in mid-summer, which is also not observed (Figs. 1B, 15a).

Sensitivity of Oyster Size and Environmental Conditions on Sporulation

Of the many assumptions made in the development of the oyster-*H. nelsoni* model, those related to sporulation are mostly based on inferences made from observations of MSX disease progression in oyster populations and corresponding changes in the host, rather than from direct observation of the process itself. One of the basic assumptions made concerns the release of density-dependent control on *H. nelsoni* growth in response to increased food levels in the spring. The sensitivity of the model to this assumption was tested by reducing the food supply in early 1965, which affects the calculation of *I factor* given by equation (16). The resulting simulation does not show an attempted sporulation event in the summer of 1965 (Fig. 16a). Rather, *H. nelsoni* prevalence remains high (BFU = 4) and about 70% of the oyster population is infected throughout the following year. In the spring of 1966, when the food levels return to the normal high values, a large attempted sporulation event occurs resulting in a sharp prevalence decline in

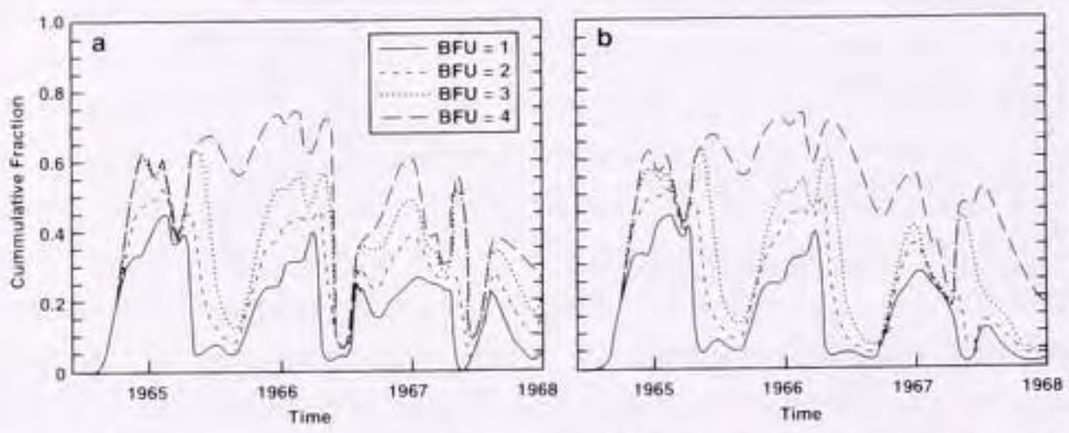

Figure 16. Simulated time-development of *Haplosporidium nelsoni* infection in BFUs (1 to 4) for a 1-g AFDW oyster in Delaware Bay after a) the oysters were exposed to low food values in 1965 and b) no spring bloom occurred in any year.

early summer. Removal of the spring bloom in all years of the simulation (Fig. 16b), disrupts the expected annual cycle completely, indicating that food supply in the spring is crucial to attempted sporulation.

Attempted sporulation events are either successful and spores are formed or unsuccessful in which case *H. nelsoni* mortality increases (Fig. 10). The difference in the two outcomes is assumed to be related to the size of the oyster. In the reference simulation (Fig. 15a), which uses a 1-g AFDW oyster, sporulation is attempted in early summer, but is unsuccessful. Parasite densities are reduced because failed sporulation leads to *H. nelsoni* death. However, *H. nelsoni* cells in a 0.3-g AFDW oyster can undergo successful sporulation and release spores (Fig. 17a). In this simulation, one successful sporulation event occurred in each of the summers of 1966 and 1967. For smaller oysters, fall sporulation is also possible (Fig. 17b), as observed (Andrews 1979, Burreson 1994). There is no *a priori* reason to expect *H. nelsoni* to attempt sporulation at only 1 or 2 times per year. In fact, when the winter temperature effect on sporulation (equation 20) is removed, small oysters can sporulate into the winter and throughout the year (Fig. 18). However, observations indicate that this does not happen and therefore some factor, such as temperature, must be restricting this process to certain times of the year.

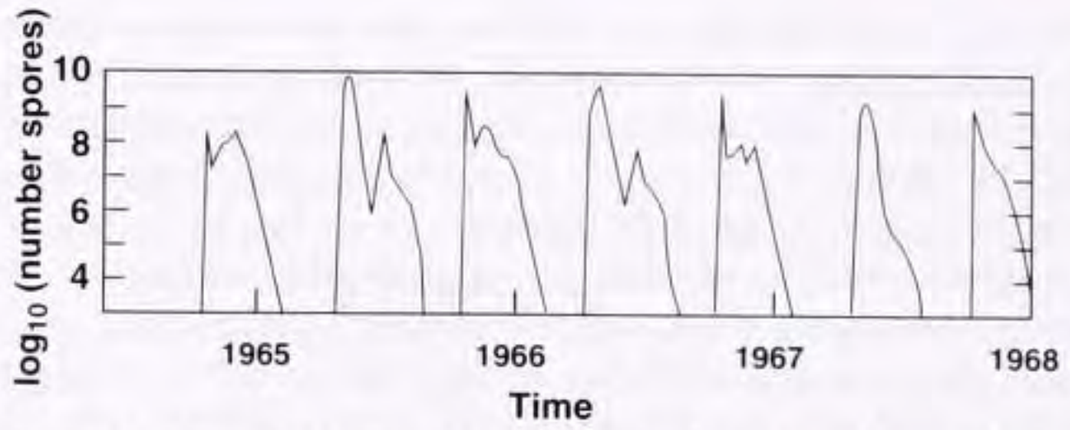

Figure 18. Simulated time-development of successful sporulation events for a 0.1-g AFDW oyster in Delaware Bay using the environmental time series from June 1964 to June 1968, representing the high-salinity lower Bay grounds. For this simulation, the winter temperature effect on *H. nelsoni* sporulation, equation (20), was removed.

Effect of Winter Temperature

Many of the relationships in the oyster-*H. nelsoni* model are dependent on winter temperature. The sensitivity of the model to these assumptions can be tested by altering the winter temperature values in the temperature time series used as input to the model. Decreasing by 50% the 1965 to 1966 winter temperatures falling below 10 °C results in a prolonged period at temperatures of 0 °C to 5 °C, which increases the number of degree days during which *H. nelsoni* is exposed to cold. The resulting simulation (Fig. 19a) shows the expected annual cycle of disease progression, although prevalence is somewhat reduced relative to the reference simulation beginning in late 1965. Because cold winters affect transmission in subsequent years (Powell et al. this volume), the major effect of the cold winter does not occur until the infection cycle beginning in the summer of 1966. Prevalences in that cycle and the following one are sharply reduced so that by the winter of 1968, only 10% of the oysters are infected. Thus, the effect of a single cold year can persist into subsequent years, even after winter temperatures have returned to normal.

The effects of a warm winter were investigated by increasing by 50% the temperatures falling below 10 °C. In this simulation, the parasites spend little time at temperatures below 5 °C and do not experience the late-winter die off (Fig. 19b). As a consequence, parasite concentrations are already high at the start of the following spring. They increase further, resulting in heavy infections in the early summer of 1966 and consequent high oyster mortality. The return to normal winter temperatures in subsequent years results in the same annual cycle as seen in the reference simulation. Thus, the effect of a single warm winter does not persist into subsequent years.

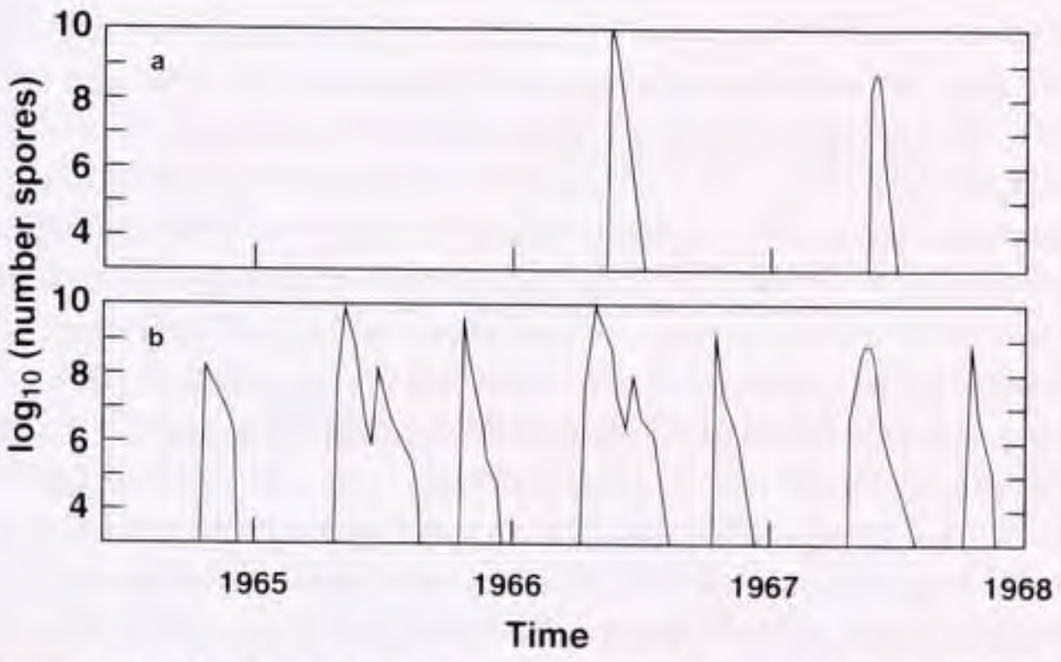

Figure 17. Simulated time-development of successful sporulation events for a) a 0.3-g AFDW oyster and b) a 0.1-g AFDW oyster in Delaware Bay using the environmental time series from June 1964 and June 1968, which represents the high-salinity, lower Bay grounds.

DISCUSSION

Model Characteristics

A numerical model describing relationships between the protistan parasite, *Haplosporidium nelsoni,* and its host, the Eastern oyster, *Crassostrea virginica,* has been developed. The model is unusually complex, particularly compared to that developed for the other major parasite of Eastern oysters, *Perkinsus marinus* (Hofmann et al. 1995, Powell et al. 1996). In the *P. marinus*-oyster model, *in vivo* parasite proliferation and death rates are a relatively simple function of temperature and salinity. Further, there is only a single life stage involved and transmission is dependent solely on the density of neighboring oysters and their infection level (Hofmann et al. 1995, Powell et al. 1996). The complexity of the *H. nelsoni* model derives from the need to consider epithelial and systemic tissues as separate compartments, the failure of the para-

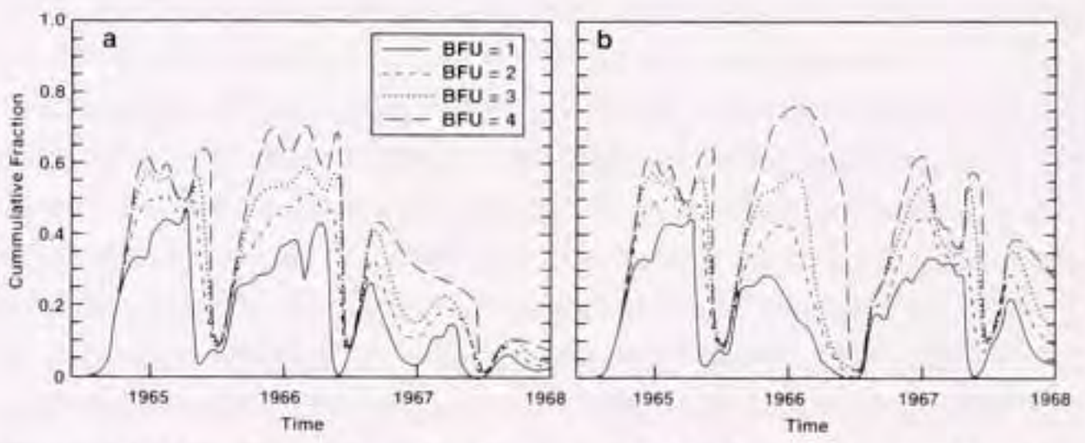

Figure 19. Simulated time-development of *Haplosporidium nelsoni* infection in BFUs (1 to 4) for a 1-g AFDW oyster in Delaware Bay with a) the winters of 1965–1966 made colder by decreasing by half the observed winter temperatures below 10 °C and b) the winter of 1965 to 1966 made warmer by increasing by half the observed winter temperatures below 10 °C.

site to respond in a straightforward way to temperature and salinity change, the need to reproduce parasite sporulation only during certain times of the year and in certain size classes of oysters, and the decoupling of transmission from host infection levels or host density. Construction of the model involved making certain assumptions about the physiological or ecological processes underlying the host-parasite relationship. Some of these assumptions are well grounded in experimental or observational data, or physiological principles; others are less so and may simply be surrogates for the true mechanism, but which happen to give the same answer. The following discussion considers these assumptions, as they occurred in the construction of the *in vivo* model. Assumptions made in the transmission component of the model are discussed in Powell et al. (this volume).

Quantifying Infection Categories

The model is quantitative; it uses parasites per oyster to track *H. nelsoni* infection development and decay. In contrast, the data used to construct and verify the model consist of semi-quantitative categories (LFU and BFU), which were converted into parasite densities by counting parasites in tissue section. Thus, a crucial assumption is that extrapolations from these counts adequately estimate total parasite burden, and that the conversion from LFUs to parasite numbers in the model is correct. In effect, the model converts from LFUs to parasite number for calculation and from parasite number back to LFUs (and then to BFUs) for data presentation. As a result, most of the constants used in the model equations are dependent upon the conversion between LFU and parasite density given by equation 1. Should that relationship change with improved quantification methods, the absolute values of most model constants would also necessarily change.

Diagnosis of *P. marinus* infections is also typically done using a semi-quantitative staging system (Mackin 1962), but a relatively accurate conversion between this system and parasite density exists and was used in construction of the *P. marinus* model (Choi et al. 1989). The *P. marinus* conversion was achieved by a process that frees the parasites from oyster tissue for counting. Plasmodial stages of *H. nelsoni* are extremely fragile and would not survive this type of manipulation. Nevertheless, some comparisons between extrapolated *H. nelsoni* densities and actual *P. marinus* counts are instructive. Estimates of *H. nelsoni* and *P. marinus* concentrations in the hemolymph of infected oysters have been made (Ford and Kanaley 1988, Ford et al. 1990, Gauthier and Fisher 1990, Bushek et al. 1994). For both parasites, maximum densities are in the range of 5×10^5 to 5×10^6 mL^{-1}. Maximum densities of *P. marinus* in soft tissues are around 10^6 parasites gwwt^{-1} (Choi et al. 1989, Bushek et al. 1994), and our estimate of peak *H. nelsoni* concentrations from tissue sections was about the same. Further, the lethal level, 10^6 parasites gwwt^{-1}, appears to be the same for both parasites, as higher densities are rarely found in live oysters. Interestingly, the estimated detection limit for *H. nelsoni* infections using tissue section histology (10^3–10^4 parasites gwwt^{-1}) is similar to the detection limit found for *P. marinus* using the standard Ray/Mackin tissue subsample method (Choi et al. 1989, Bushek et al. 1994). These values suggest fundamental similarities in the per-parasite use of nutrients from, and the damage caused to, the oyster host.

The Annual Infection Cycle within the Oyster

The estimated *in vivo* doubling times for *H. nelsoni* used in the model were 1 to 1.4 days in the systemic tissues, and 3 to 4 days in the epithelium, over the 15–25 °C range. Over the same temperature range, *P. marinus* doubling times were estimated to range between 1.3 and 2.5 days (Hofmann et al. 1995). These rates fall well within the range for most free-living and symbiotic single-celled eukaryotes (Laybourn-Parry 1987, Zaika 1973).

The *in vivo* proliferation rate of *H. nelsoni* is based on a Q_{10} of 3.2. This high value, set because lower values failed to provide adequate proliferation rates at elevated temperature, suggests that *H. nelsoni* is very sensitive to temperature change. By comparison, the Q_{10} used to model *P. marinus* cell division rates is 2.0 (Hofmann et al. 1995). Under increasing temperature, then, *H. nelsoni* doubling rates should increase faster than those of *P. marinus* and under decreasing temperatures, they should decrease faster. Over the temperature range where both parasites co-exist, approximately 0 °C to 35 °C, *H. nelsoni* has the higher proliferation rate. These comparisons of modeled proliferation rates are supported by field observations: when oysters are exposed to both parasites in the field, *H. nelsoni* begins killing before *P. marinus* does (Andrews 1967, Chintala et al. 1994).

Declining autumn temperatures failed to slow the proliferation of *H. nelsoni* sufficiently to replicate the observed plateauing of infection levels at that time of year (Andrews 1966, Ford and Haskin 1982). Consequently, it was necessary to add a crowding factor such that, at high densities, proliferation is inhibited. There is no experimental evidence that this happens in *H. nelsoni* infections, but it was also necessary to include a crowding effect in the *P. marinus* model (Hofmann et al. 1995) and there is experimental evidence that a density-dependent inhibition on proliferation does occur with this oyster parasite (Saunders et al. 1993, Ford et al. 1999). Further, a crowding effect is biologically defensible because the host is a limited resource and at some point can no longer provide enough nutrients for all parasites. For both parasites, ample evidence exists that circulating and stored nutrients are diminished by infection (Ford 1986, Barber et al. 1988, Chintala and Fisher 1991, Paynter 1996). The mechanism is analogous to cells in an *in vitro* culture, which reach a stationary phase of reduced division as culture-medium nutrients are exhausted and cellular byproducts accumulate. In the *P. marinus* and *H. nelsoni* models, crowding begins at similar parasite densities: 1 to 7×10^5 parasites gwwt^{-1}. The *P. marinus* values were obtained from empirical data as described in Hofmann et al. (1995); those for *H. nelsoni* were determined by fitting model simulations to observed MSX disease prevalence and intensity. The similarities in the threshold values for the two parasites further supports evidence presented earlier, of fundamental similarities in the amount of nutrients and the damage produced by each parasite, be it a *P. marinus* or a *H. nelsoni* cell.

The epithelium is one of the most important barriers to infection encountered by an endoparasite. Although *H. nelsoni* readily enter the epithelium, it is truly a barrier because plasmodia proliferate along the base of epithelial cells, obviously prevented from immediate entry into the circulation and often accumulating considerable parasite loads in this layer before the first subepithelial parasites are observed (Farley 1968, Ford and Haskin 1982). Infections confined to the epithelial layer are not lethal and often have few measurable effects on the oyster; further the ability to restrict parasites to the epithelium is one manifestation of resistance to MSX disease (Ford 1988, Ford and Tripp 1996). Consequently, the epithelium and the systemic tissues were considered as separate compartments in the model and the parasites behave somewhat differently in each. For instance, systemic parasites have faster division rates than do epithelial parasites, but become

crowded at lower cell densities. It was necessary to assign different proliferation rates in order to fit the model to observed infection patterns, but there is good biological rationale based on histological observation and reasoning. Myhre (1973) pointed out that in the epithelium, plasmodia are located between oyster cells. Once they have become systemic, they are continuously bathed by hemolymph. Even though the shell cavity fluid of bivalves contains dissolved proteins, indicating the availability of nutrients to a parasite lodged in this compartment, levels are approximately half that in the hemolymph (Allam and Paillard 1998, Ford unpublished). Consequently, it seems reasonable to infer that the hemolymph should provide more nutrients than the epithelium, and should allow faster multiplication. Why the crowding effects seems to run counter to this argument remains unclear, but without a higher crowding threshold in the epithelium, parasites rarely reached densities great enough to allow transfer into the systemic compartment. Although the crowding factor is based on the very plausible hypothesis of food limitation at high parasite densities, there may be another, less obvious, mechanism operating in the case of epithelial crowding.

The mechanism by which plasmodia transverse the basal lamina and enter the circulatory system is not known, although structures known as haplosporosomes, which are common in the Haplosporidia, have been postulated to contain lytic enzymes that may aid in penetration of host tissues, including the basal lamina (Perkins 1968, Scro and Ford 1990). Nevertheless, it is clear that movement of plasmodia across the basal lamina is not a simple function of parasite replication; otherwise one would not expect to see an accumulation of parasites in this layer before they appear in the subepithelial space. The approach used to model the transfer was a simple diffusion equation that depends on the concentration of parasites in both compartments. This is admittedly an artificial mechanism for transporting an organism across a membrane; however, the fact that it provided good results indicates that the true mechanism may have a similar basis. That is, the presence of large numbers of parasites is more likely to allow transfer, perhaps by weakening the basal lamina through the excretion of proteases, than is the presence of just a few plasmodia. In contrast, the *P. marinus* model does not consider the epithelium and systemic tissues as separate compartments and consequently the transfer of *P. marinus* across the epithelial barrier is a simple matter of parasite replication. The fact that this strategy works for *P. marinus,* but not for *H. nelsoni,* indicates an important difference in the way the two pathogens actually cross the barrier. In fact, it is likely that *P. marinus* is carried across within hemocytes, which routinely move between the epithelium and the circulatory system (Mackin and Boswell 1955, Alvarez et al. 1992). Thus, the chances of a phagocytosed *P. marinus* cell being carried across the basal lamina is likely to be the same for a single parasite as it is for one of many in an assemblage of parasites.

In late winter, the observed infection cycle shows a marked prevalence and intensity decline, which is considered to be a combination of the deaths of heavily infected oysters and the mortality of *H. nelsoni* plasmodia in surviving oysters (Andrews 1966, Ford and Haskin 1982). The latter is concluded from the histological appearance of plasmodia at the time. They become dense, so that it is progressively more difficult to distinguish intracellular details, then begin to stain poorly, and finally are difficult to distinguish at all. Frequently they are inside hemocytes. It is not clear what the killing mechanism is. Low temperature is an obvious candidate, but enough parasites survive to initiate a new round of infection proliferation when temperatures begin to rise in the spring (Ford 1985a). Those parasites that do survive this period apparently are lodged in the epithelium, as that is the focus of renewed proliferation activity in spring.

The initial attempt to model this observation was, in fact, to make *H. nelsoni* die as a direct result of exposure to low temperature. This strategy failed to diminish the parasite burden fast enough, as did the use of an accumulator of low temperature, degree days. The addition of host hemocyte activity against parasites made "susceptible" by prolonged (i.e., degree day) cold, reproduced, in the model, the same infection decline recorded in nature. The use of degree days does not imply that low temperature alone is causing parasite deaths. Temperature could simply be a correlate for some other condition that the parasite experiences over the winter. Ford and Haskin (1982) hypothesized that a long period of anaerobiosis with a buildup of metabolic byproducts, rather than a direct cold effect, might be deleterious to *H. nelsoni.* In fact, the presence of abundant mitochondria in the plasmodia (Scro and Ford 1990) suggested a dependence on oxidative metabolism. Whereas the mechanism causing parasite degeneration over winter is unclear, the behavior of hemocytes toward them is explainable from experimental results. Hemocytes are becoming increasingly active with rising temperatures (Fisher and Tamplin 1988). Oyster hemocytes fail to attack and phagocytose live *H. nelsoni,* but they readily ingest and eliminate parasites in the post-winter period because the plasmodia are dead or damaged (Ford et al. 1993, Ford and Ashton-Alcox 1998). Thus, the need to add to the model, for the first time, an element of host activity is entirely in accord with both observed and experimental evidence.

To fit the model to observations that declining infections persist longer in the epithelium than in the systemic tissues (Ford and Haskin 1982), systemic parasites made "susceptible" by cold are eliminated faster than those in the epithelium. Similarly, to reflect the observation that infections proliferate again from epithelial foci once temperatures begin to rise, the model sets faster recovery rates for the epithelial parasite population. This may reflect recovery of individual parasites or simply the component of undamaged parasites that remain. A possible biological explanation for the observed differences in epithelial and systemic locations is that there are probably more phagocytes per parasite in the hemolymph than in the epithelium so that the rate at which moribund parasites can be eliminated is consequently higher. Hemocyte numbers can become very high in epithelial lesions; however, they are frequently degenerate in appearance and being shed, along with parasites, into the gill cavity (Farley 1968, Ford and Tripp 1996). Differences in hemocyte-to-parasite ratios appear plausible, but there is no evidence for this hypothesis and the actual reason may be quite different.

The rate at which heavy infections decrease in late winter was observed to be slower than that for lighter infections. To model this event, it was necessary to have the overall effectiveness of the hemocyte population respond to parasite density, such that the response was relatively less effective at removing parasites at high *H. nelsoni* densities. It is reasonable that this could occur because of changing parasite-to-hemocyte ratios as infections intensify. The number of hemocytes in circulation and in tissues increases with increasing *H. nelsoni* infection intensity, but the change is relatively small (about 1.5-fold for circulating hemocytes, from a mean of 3.1×10^6 cells mL^{-1} in an uninfected oyster to a mean of 4.5×10^6 mL^{-1} in a heavily infected oyster) compared to the change in parasite concentration (from none to $>10^5$ mL^{-1}) (Ford

and Kanaley 1988, Ford et al. 1993). The disproportionate increase in parasites means that the number of *H. nelsoni* cells removed by hemocytes becomes a progressively lower proportion of the total parasite population as the number of parasites increases. Once again, it was necessary to model different rates for the systemic and epithelial tissues to reproduce observed differences. Thus, in relation to their number, epithelial hemocytes remove more parasites than do systemic hemocytes. There is no observational or experimental evidence for this model function other than the need for simulation to fit field observations of the *H. nelsoni* seasonal cycle.

Up to this point in the annual infection cycle, late winter/early spring, the model relies on temperature, parasite-density, and hemocyte activity to replicate the observed seasonal changes in parasite loads. A new element was needed, however, to explain the rapid spring infection increase from pre-existing foci, and subsequent sporulation. That element is oyster food, which remains of paramount importance throughout the remainder of the modeled annual cycle. Proliferation rates naturally increase with rising spring temperature, but the effect of temperature on parasite doubling time was inadequate to reproduce the observed, very rapid infection development in April and May. Particularly evident in field observations was the development of very heavy infections, indicating that high parasite division rates continued at densities where proliferation was otherwise restricted by self crowding. In addition to a rise in temperature in spring, the parasite experiences other changes inside the host. The oyster becomes active again after several months of quiescence over the winter. Oxygen availability rises and the accumulation of end products from anaerobic metabolism ceases. A spring bloom typically occurs, and as oyster food consumption increases, the quantity of nutrients transported in the hemolymph rises (Fisher and Newell 1986). All of these changes should provide an increasingly favorable environment for *H. nelsoni* proliferation. Further, the fact that metabolic activity and nutritional status of the oyster is increasing in the spring should provide more or better resources for the parasite, and permit higher parasite densities before crowding interferes with replication, than in late autumn when oyster metabolism is shutting down, even though nutrient reserves are generally high. Following this biological argument, the model eases the crowding effect so that higher parasite densities can be achieved rapidly in the spring. With this modification, simulations show the rapid infection intensification that occurs in the late spring and which culminates in what are often the highest parasite burdens of the year (Ford and Haskin 1982).

Nutritional status, as modeled by oyster potential growth efficiency, is equally important in the next and last phase of the annual cycle, which is the production or attempted production of spores. It is also the most complex aspect of the annual cycle model. The observation that the model needed to fit was that the late May/early June prevalence peak is relatively brief, in contrast to the winter peak, and is followed by a rapid decline in prevalence (Andrews 1966, Ford and Haskin 1982). Like the loss of infections in late winter, part of this decline is due to the deaths of heavily infected oysters and part to the loss of parasites from live oysters. To simulate this event, a second life stage, the spore, was introduced into the model. In other members of the phylum Haplosporidia, plasmodia regularly form spores (Perkins 1990), which presumably allow them to survive outside the host and are an important element in transmission. *Haplosporidium nelsoni* does form spores in adult oysters, but very rarely (Couch et al. 1966). Recent reports, however, suggest that spores are regularly formed in juvenile oysters with advanced infections (R. D. Barber et al. 1991, Burreson 1994). Spore production coincides with the May/June infection peak and also occurs as infections intensify in the fall. Sporulation takes place in the epithelium of the digestive tubules and mature spores can be shed from live oysters; however, most oysters probably die during or after the sporulation process because the overall infections are so heavy (R. D. Barber et al. 1991).

Although spores are rare in adult oysters, histological observations at the late May/early June infection peak suggest that some parasites may begin the sporulation process in adults. Oysters with advanced infections often have plasmodia in digestive tubule epithelia, sometimes with large, anomalous nuclei and a generally deteriorating appearance. We hypothesize that these plasmodia are evidence of failed sporulation, after which parasites die without completing their life cycle in the oyster. Their death consequently results in the post May/June drop in prevalence.

Observational evidence, then, suggests a difference in the environment experienced by *H. nelsoni* in young/small oysters, which allows the parasite to form spores, and that in larger/older hosts, which does not. This difference is not a question of differential susceptibility or resistance because adult oysters of both types do not support spore formation. For purposes of the model, the internal environmental quality needed for sporulation was related directly to the potential growth efficiency of the host and indirectly to food availability. Growth efficiency is an index to the amount of energy available after the host's basic metabolic requirements are met. This energy should be available to the parasite in the form of nutritional resources and relatively more of it should be available in younger oysters because of their higher growth efficiency.

Spore formation, in the model, begins with the accumulation of nutritional reserves and the accompanying intensification of infections. The parallel field observation is the movement of parasites into the digestive tubule epithelium, where they begin to undergo the many changes that accompany sporulation (Perkins 1969). The initial stages of simulated sporulation can happen regardless of oyster size, but to inhibit completion of the process in large oysters, the model establishes a threshold quantity of reserves that must be exceeded for spore production to occur. If that threshold is not reached, the process is not completed. Because of their higher growth efficiency, the threshold is exceeded only in small oysters, which consequently are the only oysters in which spores are formed. If the threshold is reached, sporulation is successful. Spores are shed from live oysters or after the host dies. The model considers that parasites that fail to sporulate are no longer viable. They become susceptible to hemocyte attack and are eliminated. In either case, resulting model simulations show a dramatic reduction in prevalence, as is seen in field observations.

The growth-efficiency basis for sporulation used by the model is hypothetical, as is failed sporulation, to explain the early summer prevalence decline in adult oysters. Some other factor, perhaps a chemical or physical "cue" having nothing to do with growth efficiency or nutritional status, may well trigger sporulation. Or, there may be a suite of elements involved that occur in juveniles only. Nevertheless, the concept of a necessary threshold of some factor or factors remains a biologically defensible generalization for the fact that *H. nelsoni* can complete its life cycle in small oysters, but rarely in large ones.

Modeling of the sporulation process needed to take into account the observation that spores are formed in juveniles in the

autumn, as well as in the spring (Andrews 1979, Burreson 1994). The process is probably set in motion in adults, too, but is rarely successful. In the fall, however, there is no abrupt prevalence decline. The model achieves this result in two ways. First, food supply is lower in the fall so only the smallest oysters have a potential growth efficiency adequate to trigger sporulation. Second, the model contains a temperature dependency on the loss of viability of plasmodia that have failed to sporulate. Thus, if sporulation fails at relatively low temperature, plasmodia become less susceptible to hemocyte attack than those failing at relatively high temperature. Oysters remain infected and eventually die in late winter. In fact, if the "internal environment cue" hypothesis is correct and is related to the accumulation of nutrients, the slower reserve build up in adults compared to juveniles may simply retard the spore-formation process until the temperature is too low for parasite activity, so the plasmodia are never damaged.

Salinity Effects

Temperature is undoubtedly the most important environmental variable influencing the seasonal infection cycle, both directly and indirectly, and in the field and in the model. Salinity is also important, but its effect is more obvious when considered on spatial or long-term temporal scales (Paraso et al. this volume, Powell et al. this volume). In the model, salinity affects *H. nelsoni* inside the oyster by affecting both survival and proliferation rates. Both are parameterized from *in vitro* experiments describing survival of plasmodia after acute salinity change (Ford and Haskin 1988). Results of these trials showed that survival was very low below about 9 ppt and very high above about 15 ppt, which roughly approximates its distribution in nature (Ford and Tripp 1996). Between those ranges, the parasite is highly sensitive to small salinity change. The model also considers that inside the oyster, parasites are buffered from rapid changes in salinity by the behavior of oysters themselves. When exposed to a large salinity change, bivalves typically close their valves and thereafter open them only briefly so as to allow entry of only small amounts of ambient water (Schoffeniels and Gilles 1972, Davenport 1979). The salt content of their body fluid thus changes more slowly than does the external water. Consequently, the model extends the *in vitro* death rate over a period of 4 days. In the absence of data on the effect of salinity on *in vivo* doubling times, it seems reasonable to assume that the salinity range over which it occurs is roughly the same as for survival, and that within this range, the response pattern is similar.

In the model, salinity also affects the rate at which parasites move into the systemic tissue from the epithelium: at low salinity, the rate increases. This was a way to maintain the constant ratio of systemic to local infections observed along the salinity gradient (Haskin and Ford 1982, Fegley et al. 1994). Without it, the frequency of systemic infections decreased with decreasing salinity. Low salinity may, in fact, make it easier for parasites to make this transition, although the physiological mechanism is unclear. The actual reason may be quite different and this may be a case where the mathematical device provided a good approximation of observed patterns without a good biological rationale. Nevertheless, the need to include a factor that increased the proportion of systemic infections indicates that a simple salinity effect on parasite survival and growth is not sufficient to explain what is observed in field data.

Oyster Mortality

Oysters die, in the model, when *H. nelsoni* densities exceed that which is seen in live oysters. The same is true for the *P. marinus* model, but the *H. nelsoni* model also reflects the fact that the lethal parasite density for some oysters is lower than this maximally observed level. A few individuals die with relatively light infections and an increasing proportion die as infections intensify. It is this variation in ability to tolerate infections that forms one of the bases for selective breeding: comparisons between oyster strains selected and unselected for resistance to MSX disease indicate that one measure of resistance is the ability to survive with relatively heavy infections (Ford and Haskin 1987, Ford 1988, B. J. Barber et al. 1991).

Transmission

Incomplete knowledge of the life cycle and mechanism of transmission of *H. nelsoni* is probably the single greatest impediment to further understanding this important parasite and the disease it causes. The sparsity of information about transmission made modeling this aspect of MSX disease particularly difficult because many assumptions had to be made. Yet the exercise was both intriguing and insightful. The transmission model is a separate component of the overall *H. nelsoni*-oyster model. It differs from most transmission models in that it simulates success or failure of transmission based on external environmental factors rather than on the density and infection levels of neighboring oysters. Modeling of the transmission process is detailed and discussed by Powell et al. (this volume).

SUMMARY

The component of the *H. nelsoni* model that describes host-parasite interactions inside the oyster is constructed using functions describing physiological rates for both organisms: proliferation, translocation, and death (or degradation) of the parasite; and hemocyte activity, filtration rate, and growth efficiency of the oyster. The rates, in turn, are controlled by four environmental variables: temperature, salinity, food, and total seston. Using only these few elements, the model is able to reproduce the bimodal annual infection cycle that includes infection intensification and remission, a life stage change of the parasite, response of the oyster's internal defense system, and, eventually, oyster death. With few exceptions, the physiological rate functions are based on experimental or observational evidence or general physiological principles. For instance, the effect of salinity on *in vivo* parasite survival, and the response of oyster hemocytes to dead or damaged parasites is well grounded with experimental, as well as observational, data (Haskin and Ford 1982, Fisher and Tamplin 1988, Ford and Haskin 1988, Ford et al. 1993, Ford and Ashton-Alcox 1998). Parasite doubling times and the relationship between oyster mortality and infection intensity were computed directly from field data (Andrews 1966, Ford and Haskin 1982). Physiologically well-reasoned arguments were made for the self-crowding effect, the release of crowding in the spring, parasite degradation over the winter, differences in parasite growth and death rates between epithelial and systemic compartments, and the "threshold" trigger for sporulation. Whether failed sporulation in adult oysters is the cause for the rapid prevalence decline after the spring infection peak, whether lower salinity facilitates the movement of parasites from the epithelium into the systemic tissues, and the increased "efficiency" of the hemocyte component in the epithelium are

highly conjectural. Because virtually nothing is known about the transmission mechanism, this component of the model includes more hypothetical elements: specifically the infective dose threshold and the concentration of infective particles and their relationship to salinity and temperature (Powell et al. this volume).

The fact that certain hypothetical mechanisms were used to fit the model to observation does not detract from its efficacy. Because the simulations reproduce observed temporal and spatial patterns, and assuming that the major biological and physical systems involved have, at some level, reasonably predictable responses, the model suggests ways in which the host-parasite system must work. For instance, the modeling exercise clearly shows that temperature effects on parasite doubling times or salinity effects on *in vivo* parasite survival, cannot by themselves, explain field observations. The model demonstrates that other factors must be involved and points to where efforts must be concentrated to gain a better understanding of the overall host-parasite relationship. Clearly, an improved knowledge of the complete system rests with a better understanding of the parasite's life cycle and mode of transmission, combined with an ability to infect oysters experimentally. Nevertheless, the fact that this very complex and detailed model works, with few modifications, in Chesapeake Bay as well as in Delaware Bay, is a measure of its power and potential usefulness in other areas.

ACKNOWLEDGMENTS

We thank Bob Barber at HSRL for examination of oysters to provide the LFU-to-parasite abundance relationship. This research was supported by the Virginia Graduate Marine Science Consortium grant VGMSC 5-29222 and by the New Jersey Sea Grant under contract number 4-25238. Computer resources and facilities were provided by the Center for Coastal Physical Oceanography at Old Dominion University. The Delaware River and Bay Authority funded the 1981–1984 monitoring program that provided data for some of the environmental time series used in the model. Continuation of the time series through 1986 was made possible by funds from the New Jersey Department of Environmental Protection. Both programs were coordinated by Walt Canzonier. The States of New Jersey and Maryland provided funds for collection of the Delaware Bay and Chesapeake Bay *Haplosporidium nelsoni* time series. This is Contribution number 99-16 of the Institute of Marine Science at Rutgers University and NJAES Publication #D-32405-1-99.

LITERATURE CITED

Allam, B. & C. Paillard. 1998. Defense factors in clam extrapallial fluids. *Dis. Aquat. Org.* 33:123–128.

Alvarez, M. R., F. E. Friedl, C. M. Hudson & R. L. O'Neill. 1992. Uptake and tissue distribution of abiotic particles from the alimentary tract of the American oyster: A simulation of intracellular parasitism. *J. Invertebr. Pathol.* 59:290–294.

Alvarez, M. R., F. E. Friedl, J. S. Johnson & G. W. Hinsch. 1989. Factors affecting *in vitro* phagocytosis in oyster hemocytes. *J. Invertebr. Pathol.* 54:233–241.

Andrews, J. D. 1966. Oyster mortality studies in Virginia. Epizootiology of MSX, a protistan parasite of oysters. *Ecology* 47:19–31.

Andrews, J. D. 1967. Interaction of two diseases of oysters in natural waters. *Proc. Natl. Shell. Assoc.* 57:38–48.

Andrews, J. D. 1968. Oyster mortality studies in Virginia. VII. Review of epizootiology and origin of *Minchinia nelsoni*. *Proc. Natl. Shellfish. Assoc.* 58:23–36.

Andrews, J. D. 1979. Oyster diseases in Chesapeake Bay. *Mar. Fish. Rev.* 41:45–53.

Andrews, J. D. 1983. *Minchinia nelsoni* (MSX) infections in the James River seed-oyster area and their expulsion in spring. *Estuarine, Coastal and Shelf Sci.* 16:255–269.

Barber, B. J., S. E. Ford & H. H. Haskin. 1988. Effects of the parasite MSX (*Haplosporidium nelsoni*) on oyster (*Crassostrea virginica*) energy metabolism. II. Tissue biochemical composition. *Comp. Biochem. Physiol.* 91A:603–608.

Barber, B. J., S. E. Ford & D. T. J. Littlewood. 1991. A physiological comparison of resistant and susceptible oysters *Crassostrea virginica* (Gmelin), exposed to the endoparasite, *Haplosporidium nelsoni* (Haskin, Stauber, and Mackin). *J. Exp. Mar. Biol. Ecol.* 146:101–112.

Barber, B. J., R. R. Langan & T. L. Howell. 1997. *Haplosporidium nelsoni* (MSX) epizootic in the Piscataqua River Estuary (Maine/New Hampshire, U.S.A.). *J. Parasitol.* 83:148–150.

Barber, R. D. & S. E. Ford. 1992. Occurrence and significance of ingested haplosporidan spores in the eastern oyster, *Crassostrea virginica* (Gmelin, 1791). *J. Shellfish Res.* 11:371–375.

Barber, R. D., S. A. Kanaley & S. E. Ford. 1991. Evidence for regular sporulation by *Haplosporidium nelsoni* (MSX) (Ascetospora: Haplosporidiidae) in spat of the American oyster, *Crassostrea virginica*. *J. Protozool.* 38:305–306.

Burreson, E. M. 1988. Use of immunoassays in haplosporidan life cycle studies. pp. 298–303. *In:* W. S. Fisher (ed.). Disease Processes in Marine Bivalve Molluscs. Spec. Pub. 18, Am Fish Soc, Bethesda, MD.

Burreson, E. M. 1994. Further evidence of regular sporulation by *Haplosporidium nelsoni* in small oysters, *Crassostrea virginica*. *J. Parasitol.* 80:1036–1038.

Bushek, D., S. E. Ford & S. K. Allen. 1994. Evaluation of methods using Ray's fluid thioglycollate medium for diagnosis of *Perkinsus marinus* infection in the eastern oyster, *Crassostrea virginica*. *Ann. Rev. Fish Diseases* 4:201–217.

Chintala, M. M. & W. S. Fisher. 1991. Disease incidence and potential mechanisms of defense for MSX-resistant and susceptible eastern oysters held in Chesapeake Bay. *J. Shellfish Res.* 10:439–443.

Chintala, M. M., S. E. Ford, W. S. Fisher & K. A. Ashton-Alcox. 1994. Oyster serum agglutinins and resistance to protozoan parasites. *J. Shellfish Res.* 13:115–121.

Choi, K.-S., E. A. Wilson, D. H. Lewis, E. N. Powell & S. M. Ray. 1989. The energetic cost of *Perkinsus marinus* parasitism in oysters. Quantification of the thioglycollate method. *J. Shellfish Res.* 8:117–125.

Corliss, J. O. 1984. The kingdom Protista and its 45 phyla. *BioSystems* 17:87–126.

Couch, J. A., C. A. Farley & A. Rosenfield. 1966. Sporulation of *Minichinia nelsoni* (Haplosporida, Haplosporidiidae) in *Crassostrea virginica* (Gmelin). *Science* 153:1529–1531.

Davenport, J. 1979. Is *Mytilus edulis* a short term osmoregulator? *Comp. Biochem. Physiol.* 64A:91–95.

Farley, C. A. 1968. *Minchinia nelsoni* (Haplosporida) disease syndrome in the American oyster *Crassostrea virginica*. *J. Protozool.* 15:585–599.

Farley, C. A. 1975. Epizootic and enzootic aspects of *Minchinia nelsoni* (Haplosporida) disease in Maryland oysters. *J. Protozool.* 22:418–427.

Fegley, S. R., S. E. Ford, J. N. Kraeuter & D. R. Jones. 1994. Relative effects of harvest pressure and disease mortality on Eastern Oyster population dynamics in Delaware Bay. Final Report to NOAA, NMFS Oyster Disease Research Program. Rutgers, The State University of New Jersey. 208 pp.

Feng, S. Y. & J. S. Feng. 1974. The effect of temperature on cellular reactions of *Crassostrea virginica* to the injection of avian erythrocytes. *J. Invertebr. Pathol.* 23:22–37.

Fisher, W. S. & R. I. E. Newell. 1986. Seasonal and environmental varia-

tion in the protein and carbohydrate levels in the hemolymph from American oysters (*Crassostrea virginica* Gmelin). *Comp. Biochem. Physiol.* 85A:365–372.

Fisher, W. S. & M. Tamplin. 1988. Environmental influence on activities and foreign-particle binding by hemocytes of American oysters, *Crassostrea virginica*. *Can. J. Fish. Aquat. Sci.* 45:1309–1315.

Ford, S. E. 1985a. Chronic infections of *Haplosporidium nelsoni* (MSX) in the oyster *Crassostrea virginica*. *J. Invertebr. Pathol.* 45:94–107.

Ford, S. E. 1985b. Effects of salinity on survival of the MSX parasite *Haplosporidium nelsoni* (Haskin, Stauber, and Mackin) in oysters. *J. Shellfish Res.* 2:85–90.

Ford, S. E. 1986. Comparison of hemolymph proteins between resistant and susceptible oysters, *Crassostrea virginica*, exposed to the parasite *Haplosporidium nelsoni* (MSX). *J. Invertebr. Pathol.* 47:283–294.

Ford, S. E. 1988. Host parasite interactions in oysters, *Crassostrea virginica*, selected for resistance to *Haplosporidium nelsoni* (MSX) disease: survival mechanisms against a natural pathogen. pp. 206–224. *In:* W. S. Fisher, (ed.). Disease Processes in Marine Bivalve Molluscs. Spec. Pub. 18, Am. Fish. Soc., Bethesda, MD.

Ford, S. E. 1996. Range extension by the oyster parasite *Perkinsus marinus* into the northeastern US: response to climate change? *J. Shellfish Res.* 15:45–56.

Ford, S. E. & K. A. Ashton-Alcox. 1998. Altered response of oyster hemocytes to *Haplosporidium nelsoni* (MSX) plasmodia treated with enzymes or metabolic inhibitors. *J. Invertebr. Pathol.* 72:160–166.

Ford, S. E. & H. H. Haskin. 1982. History and epizootiology of *Haplosporidium nelsoni* (MSX), an oyster pathogen, in Delaware Bay, 1957–1980. *J. Invertebr. Pathol.* 40:118–141.

Ford, S. E. & H. H. Haskin. 1987. Infection and mortality patterns in strains of oysters *Crassostrea virginica* selected for resistance to the parasite *Haplosporidium nelsoni* (MSX). *J. Parasitol.* 73:368–376.

Ford, S. E. & H. H. Haskin. 1988. Comparison of *in vitro* salinity tolerance of the oyster parasite *Haplosporidium nelsoni* (MSX) and hemocytes from the host, *Crassostrea virginica*. *Comp. Biochem. Physiol.* 90A: 183–187.

Ford, S. E. & S. A. Kanaley. 1988. An evaluation of hemolymph diagnosis for detection of the oyster parasite *Haplosporidium nelsoni* (MSX). *J. Shellfish Res.* 7:11–18.

Ford, S. E., S. A. Kanaley & K. A. Ashton-Alcox. 1993. *In vitro* interactions between bivalve hemocytes and the oyster pathogen *Haplosporidium nelsoni* (MSX). *J. Parasitol.* 79:255–265.

Ford, S. E., S. A. Kanaley, M. Ferris & K. A. Ashton-Alcox. 1990. "Panning," a technique for enrichment of the parasite *Haplosporidium nelsoni* (MSX) from hemolymph of infected oysters. *J. Invertebr. Pathol.* 56:347–352.

Ford, S. E., A. Schotthoefer & C. Spruck. 1999. *In vivo* dynamics of the microparasite *Perkinsus marinus* during progression and regression of infections in eastern oysters. *J. Parasitol.* 85:273–282.

Ford, S. E. & M. R. Tripp. 1996. Diseases and defense mechanisms. pp. 383–450. *In:* R. I. E. Newell, V. S. Kennedy and A. F. Eble (eds.). The Eastern Oyster *Crassostrea virginica*. Maryland Sea Grant College, College Park, MD.

Galtsoff, P. S. 1964. The America Oyster, *Crassostrea virginica* Gmelin. United States Department of the Interior, Washington, D.C. 480 pp.

Gauthier, J. D. & W. S. Fisher. 1990. Hemolymph assay for diagnosis of *Perkinsus marinus* in oysters *Crassostrea virginica* (Gmelin, 1791). *J. Shellfish Res.* 9:367–372.

Haskin, H. H. 1972. Delaware River flow-bay salinity relationships. Report to the Delaware River Basin Commission: Phase III. 12 pp.

Haskin, H. H. & J. D. Andrews. 1988. Uncertainties and speculations about the life cycle of the eastern oyster pathogen *Haplosporidium nelsoni* (MSX). pp. 5–22. *In:* W. S. Fisher (ed.). Disease Processes in Marine Bivalve Molluscs. Spec. Pub. 18, Am. Fish. Soc., Bethesda, MD.

Haskin, H. H. & S. E. Ford. 1982. *Haplosporidium nelsoni* (MSX) on Delaware Bay seed oyster beds: a host-parasite relationship along a salinity gradient. *J. Invertebr. Pathol.* 40:388–405.

Hofmann, E. E., J. M. Klinck, E. N. Powell, S. Boyles & M. Ellis. 1994. Modeling oyster populations II. Adult size and reproductive effort. *J. Shellfish Res.* 13:165–182.

Hofmann, E. E., E. N. Powell, J. M. Klinck & G. Saunders. 1995. Modeling diseased oyster populations I. Modeling *Perkinsus marinus* infections in oysters. *J. Shellfish Res.* 14:121–151.

Hofmann, E. E., E. N. Powell, J. M. Klinck & E. A. Wilson. 1992. Modeling oyster populations III. Critical feeding periods, growth and reproduction. *J. Shellfish Res.* 11:399–416.

Laybourn-Parry, J. 1987. Protozoa. pp. 1–25. *In:* T. J. Pandian and F. J. Vernberg (eds.). *Animal Energetics*. vol. 1. *Protozoa through Insecta*. Academic Press, New York.

Mackin, J. G. 1962. Oyster diseases caused by *Dermocystidium marinum* and other microorganisms in Louisiana. pp. 132–229. *In:* J. G. Mackin and S. H. Hopkins (eds.). *Studies on Oysters in Relation to the Oil Industry*. 7. Publication of the Institute of Marine Science, Texas A&M University.

Mackin, J. G. & J. L. Boswell. 1955. The life cycle and relationships of *Dermocystidium marinum*. *Proc. Natl. Shellfish. Assoc.* 46:112–115.

Matthiessen, G. C., S. Y. Feng & L. Leibovitz. 1990. Patterns of MSX (*Haplosporidium nelsoni*) infection and subsequent mortality in resistant and susceptible strains of the eastern oyster *Crassostrea virginica* (Gmelin, 1791) in New England. *J. Shellfish Res.* 9:359–366.

Myhre, J. L. 1973. Levels of infection in spat of *Crassostrea virginica* and mechanisms of resistance to the haplosporidian parasite *Minchinia nelsoni*. M. S. Rutgers University, New Brunswick, NJ. 102 pp.

Paraso, M. C, S. E. Ford, E. N. Powell, E. E. Hofmann & J. M. Klinck. 1999. Modeling the MSX parasite in eastern oyster (*Crassostrea virginica*) populations. II. Salinity effects. *J. Shellfish Res.*

Paynter, K. T. 1996. The effects of *Perkinsus marinus* infection on physiological processes in the eastern oyster, *Crassostrea virginica*. *J. Shellfish Res.* 15:119–125.

Perkins, F. O. 1968. Fine structure of the oyster pathogen *Minchinia nelsoni* (Haplosporida, Haplosporidiidae). *J. Invertebr. Pathol.* 10:287–307.

Perkins, F. O. 1969. Electron microscope studies of sporulation in the oyster pathogen, *Minchinia costalis* (Sporozoa; Haplosporida). *J. Parasitol.* 55:897–920.

Perkins, F. O. 1990. Phylum Haplosporidia. pp. 19–29. *In:* L. Margulis, J. O. Corliss, M. Melkonian and D. J. Chapman (eds.). Handbook of Protoctista. Jones and Bartlett, Boston.

Powell, E. N., E. E. Hofmann & J. M. Klinck. 1996. Modeling diseased oyster populations II. Triggering mechanisms for *Perkinsus marinus* epizootics. *J. Shellfish Res.* 15:141–165.

Powell, E. N., J. M. Klinck, S. E. Ford, E. E. Hofmann & S. J. Jordan. 1999. Modeling the MSX parasite in eastern oyster (*Crassostrea virginica*) populations. III. Regional application and the problem of transmission. *J. Shellfish Res.* 18:515–536.

Powell, E. N., J. M. Klinck, E. E. Hofmann & S. E. Ford. 1997. Varying the timing of oyster transplant: implications for management from simulation studies. *Fish. Oceanog.* 6:213–237.

Powell, E. N., J. M. Klinck, E. E. Hofmann & S. M. Ray. 1994. Modeling oyster populations IV. Rates of mortality, population crashes, and management. *Fishery Bull.* 92:347–373.

Ray, S. M. 1996. Historical perspsective on *Perkinsus marinus* disease of oysters in the Gulf of Mexico. *J. Shellfish Res.* 15:9–11.

Saunders, G. L., E. N. Powell & D. H. Lewis. 1993. A determination of *in vivo* growth rates for *Perkinsus marinus*, a parasite of *Crassostrea virginica*. *J. Shellfish Res.* 12:229–240.

Soniat, T. M., E. N. Powell, E. E. Hofmann, & J. M. Klinck. 1998. Understanding the success and failure of oyster populations: the importance of sampled variables and sample timing. *J. Shellfish Res.* 17:1149–1165.

Schoffeniels, E. & R. Gilles. 1972. Ion-regulation and Osmoregulation in Mollusca. pp. 393–420. *In:* M. Florkin and B. T. Scheer (eds.). Chemical Zoology. vol. 7: Mollusca. Academic Press, New York.

Scro, R. A. & S. E. Ford. 1990. An electron microscope study of disease progression in the oyster *Crassostrea virginica* infected with the protozoan parasite *Haplosporidium nelsoni* (MSX). pp. 229–254. *In:* F. O. Perkins and T. C. Cheng (eds.). Pathology in Marine Science. Academic Press, Orlando, FL.

Shumway, S. E. 1996. Natural Environmental Factors. pp. 467–513. *In:* R. I. E. Newell, V. S. Kennedy and A. F. Eble (eds.). The Eastern Oyster *Crassostrea virginica.* Maryland Sea Grant College, College Park, MD.

Sprague, V., E. A. Dunnington & E. Drobeck. 1969. Decrease in incidence of *Minchinia nelsoni* in oysters accompanying reduction of salinity in the laboratory. *Proc. Natl. Shellfish. Assoc.* 59:23–26.

Stokes, N. A., M. E. Siddall & E. M. Burreson. 1995. Detection of *Haplosporidium nelsoni* (Haplosporidia: Haplosporidiidae) in oysters by PCR amplification. *Dis. Aquat. Org.* 23:145–152.

Verwer, J. G. & M. van Loon. 1994. An evaluation of explicit pseudo-steady-state approximation schemes for stiff ODE systems from chemical kinetics. *J. Comput. Phys.* 113:347–352.

Zaika, V. E. 1973. Specific Production of Aquatic Invertebrates. John Wiley & Sons, New York, 154 pp.